

**CHITOSAN-PLASMID DNA NANOPARTICLES:
CYTOTOXIC AND CYTOSTATIC EFFECTS ON
HUMAN CELL LINES**

**A Thesis Submitted to
the Graduate School of Engineering and Sciences of
İzmir Institute of Technology
in Partial Fulfillment of the Requirements for the Degree of**

MASTER OF SCIENCE

in Biotechnology

**by
Gizem BOR**

**December 2015
İZMİR**

We approve the thesis of **Gizem BOR**

Examining Committee Members:

Assoc. Prof. Dr. Gülşah ŞANLI

Department of Chemistry, İzmir Institute of Technology

Prof. Dr. Şenay ŞANLIER

Department of Biochemistry, Ege University

Assoc. Prof. Dr. Hüseyin Çağlar KARAKAYA

Department Molecular Biology and Genetis , İzmir Institute of Technology

25 December 2015

Assoc. Prof. Dr. Gülşah ŞANLI

Supervisor, Department of Chemistry
İzmir Institute of Technology

Prof. Dr. Mustafa M. DEMİR

Co-Supervisor, Department of Materials
Science and Engineering
İzmir Institute of Technology

Prof. Dr. Volga BULMUŞ

Head of the Department of Biotechnology
and Bioengineering

Prof. Dr. Bilge KARAÇALI

Dean of the Graduate School of
Engineering and Sciences

ACKNOWLEDGMENTS

First of all, I would like to express my deepest gratitude to my advisor, Assoc. Prof. Dr. Gülşah ŞANLI, for her excellent guidance, smiling face, patience, and humour, friendship, openness and inspiration. It has been great honour to be her M.Sc. student and work with such a wonderful person.

I would like to extend a note of thanks to Dr. Maciej WNUK, who helping me at University of Rzeszów with an excellent atmosphere for doing research. I appreciate all his contributions of time, ideas, and providing my ERASMUS experience productive and stimulating. I would never have been able to finish my work without the guidance of him. Moreover, his team has been a source of friendships as well as good advice and collaboration. I am especially grateful to Anna LEWINSKA, Jennifer MYTYCH, Jagoda ADAMCZYK and others who were always so helpful and provided me with their assistance throughout my research. *Dziękuję wszystkim szczerze!*

My time at IZTECH was made enjoyable in large part due to the many friends and laboratory members that became a part of my life. I would like to thank to my friends Ayça ZEYBEK, Murat DELMAN, Burcu ÖZDAMAR, Müge ALGAN and Yasin ÖZ for encouragements and constructive comments during my studies and also having good times during coffee breaks.

My deep appreciation goes out to M. Çağrı CEYLAN, who kindly and patiently helped me with so many computer issues. Furthermore, his support, peacefulness, encouragement and assistance were also a great help to me during this challenging period.

I would also like to say a heartfelt thank you to my parents, Nesrin and Mustafa BOR, for all their continuous support and endless love. Special gratitude is devoted to my sister, Aslı BOR TÜRKBEN, and her husband, A. Levent TÜRKBEN, for believing in me and encouraging me to follow my dreams. Finally, I would like to give a special thanks to my all other extend family members for their love and support, which always inspired me through my research.

ABSTRACT

CHITOSAN-PLASMID DNA NANOPARTICLES: CYTOTOXIC AND CYTOSTATIC EFFECTS ON HUMAN CELL LINES

Although chitosan nanoparticles (CNs) became a promising tool for several biological and medical applications owing to their inherent biocompatibility and biodegradability, studies regarding their effects on cytotoxicity and cytostatic properties still remain insufficient.

Therefore, in the present study, we decided to perform comprehensive analysis of the interactions between CNs – pKindling-Red-Mito (pDNA) and different cell line models derived from blood system and human solid tissues cancers. The resulting CNs-pDNA was investigated with regard to their physical-chemical properties, cellular uptake and transfection efficiency, cytotoxic and cytostatic properties. The nanoparticles showed high encapsulation efficiency and physical stability even after 2 days for various formulations. Moreover, high gene expression levels were observed already 96 h after transfection. CNs-pDNA treatment, despite the absence of oxidative stress induction, caused cell cycle arrest in G0/G1 phase and as consequence led to premature senescence, which turned out to be both, p21-dependent and p21-independent. Also, observed DNMT2 upregulation may suggest the activation of different pathways protecting from the resulting CNs-mediated stress. In conclusion, treatment of different cell lines with CNs-pDNA showed that their biocompatibility was limited and effects were cell type-dependent.

ÖZET

KİTOSAN-PLAZMİD DNA NANOPARÇACIKLARI: İNSAN HÜCRE HATLARI ÜZERİNE SİTOTOKSİK VE SİTOSTATİK ETKİLERİ

Kitosan nanoparçacıklar (CNs), kendi doğasında olan biyouyumluluk ve biyo-çözünürlülük özellikleri nedeniyle birçok biyolojik ve tıbbi uygulamalarda gelecek vaat eden bir araç olmasına rağmen, sitotoksik ve sitostatik özellikleri üzerindeki etkileri ile ilgili çalışmalar yetersiz kalmaktadır.

Bu sebeple, bu çalışmada, CNs – pKindling-Red-Mito (pDNA) ve farklı hücre hatları arasındaki etkileşimlerin kapsamlı bir analizini gerçekleştirmeye karar verdik. Elde edilen kitosan-plasmid DNA nanoparçacıkları; hücre alımı, transfeksiyon verimi, fiziksel-kimyasal özellikleri, sitotoksik ve sitostatik etkileri bakımından incelenmiştir. Nanoparçacıklar, sentezlenen çeşitli formülasyonları için 2 gün sonrasında bile yüksek enkapsülasyon etkinliği ve fiziksel stabilite göstermiştir. Diğer taraftan, gen ekspresyonu, transfeksiyonun 96 saat sonrasında yüksek düzeyde gözlenmiştir. CNs-pDNA muamelesi, oksidatif stres indüksiyonunun yokluğu rağmen, G0 / G1 fazında hücre döngüsünün baskılanmasına sebep olmakta ve sonuç olarak, hem p21-bağımlı hem de p21-bağımsız olarak ortaya çıkan erken senesense neden olmuştur. Ayrıca, gözlemlenen DNMT2 upregülasyonu, oluşan CNs-kaynaklı stresi önleyici farklı yollarının aktivasyonu hakkında fikir verebilir. Sonuç olarak, CNs-pDNA ile muamele edilmiş farklı hücre hatları, parçacıkların sınırlı biyo-uyumluluğunun olduğunu ve etkilerinin hücre tipine-bağlı olduğunu göstermiştir.

TABLE OF CONTENTS

LIST OF FIGURES	ix
LIST OF TABLES	xi
LIST OF ABBREVIATIONS	xii
CHAPTER 1. INTRODUCTION	1
CHAPTER 2. LITERATURE REVIEW	3
2.1. Gene Therapy	3
2.1.1. Gene Transfer Methods	4
2.1.2. Plasmid DNA Based Therapeutics	5
2.2. Chitosan	5
2.2.1. Chemical Structure of Chitin and Chitosan	6
2.2.2. Biological Properties of Chitosan	8
2.3. Chitosan as a Non-viral Vector	9
2.4. Barriers for Cellular Delivery of Non-viral Vectors	12
2.4.1. Extracellular Barriers	12
2.4.2. Intracellular Barriers	13
2.5. Cytotoxicity and Nanomaterials	14
CHAPTER 3. MATERIALS AND METHODS	16
3.1. Materials	16
3.2. Methods	17
3.2.1. Preparation of Bacterial Plasmids	17
3.2.2. Synthesis of Chitosan Nanoparticles by Ionic Gelation Method ..	18
3.2.3. Synthesis of Chitosan-pDNA Nanoparticles (CNs-pDNA)	19
3.2.4. Techniques for Characterization of CNs-pDNA Particles	20
3.2.5. Determination of pDNA Encapsulation Efficiency	23
3.2.6. Evaluation of CNs-pDNA Integrity	24
3.2.7. <i>In vitro</i> Studies	24

3.2.7.1. Cell Cultures	24
3.2.7.2. Passaging of Cell Lines.....	25
3.2.7.3. Freezing and Thawing Cultured Cells	26
3.2.7.4. Cell Proliferation, Cytotoxicity and Cell Cycle Analysis.....	26
3.2.7.5. <i>In Vitro</i> Transfection Studies.....	27
3.2.7.6. Senescence-associated β -galactosidase activity (SA- β -gal)	28
3.2.7.7. Oxidative Stress	29
3.2.7.8. TUNEL Assay.....	29
3.2.7.10. Total Protein Extraction from the Cells.....	30
3.2.7.11. Determination of Protein Concentration by BCA Assay.....	30
3.2.7.12. Western Blotting	31
3.8. Statistical Analysis.....	32
CHAPTER 4. RESULTS AND DISCUSSION.....	33
4.1. Formation and Optimization of Chitosan Nanoparticles	33
4.1.1. Effect of CS:TPP Mass Ratio	34
4.1.2. Effect of pH	35
4.2. Synthesis and Characterization of Chitosan-plasmid DNA Nanoparticles (CNs-pDNA)	37
4.3. Transfection Efficiency of CNs-pDNA	39
4.4. Cell type-dependent Cytotoxic and Cytostatic Effect of CNs and CNs-pDNA	44
4.5. Oxidative stress-induced premature senescence.....	49
CHAPTER 5. CONCLUSION	56
REFERENCES..	58
APPENDICES	
APPENDIX A. MEDIA AND BUFFERS FOR THE TRANSFORMATION OF pKINDLING-RED-MITO	68
APPENDIX B. MEDIA AND SOLUTIONS FOR <i>IN VITRO</i> STUDIES	70

APPENDIX C. REAGENTS AND SOLUTIONS FOR THE DETERMINATION OF THE SENESENCE-ASSOCIATED β -GALACTOSIDASE ACTIVITY (SA- β -gal)	71
APPENDIX D. REAGENTS AND GEL PREPARATION FOR WESTERN BLOTTING	72

LIST OF FIGURES

Figure	Page
Figure 2.1. The basic of gene delivery systems for gene therapy.....	4
Figure 2.2. Schematic representation of Chitosan manufacturing process from Chitin...	8
Figure 2.3. Functional groups of chitosan	7
Figure 2.4. The drawbacks of chitosan as non-viral vector.	9
Figure 2.5. Schematic representation of the main methods for formulating chitosan based nanoparticles for nucleic acid delivery	11
Figure 2.6. Mainly extra- and intracellular barriers for non-viral gene delivery.....	14
Figure 3.1. Schematic presentation of pKindling-Red-MitoVector.....	17
Figure 3.2. Schematic illustration of the chitosan nanoparticle formulation.....	19
Figure 3.3. Schematic illustration of the chitosan plasmid DNA nanoparticle (CNs-pDNA) formulation.....	20
Figure 3.4. Smaller particles cause the intensity to fluctuate more rapidly than large particles in DLS measurements	21
Figure 3.5. (A) Representation of the relation between surface charge and zeta potential value. (B) Principles of LDV in measuring the zeta potential.....	22
Figure 3.6. Basic principles of Atomic Force Microscopy.....	23
Figure 3.7. Microscope images of HeLa, MDA-MB-231 and THP-1 cell lines.	25
Figure 3.8. Mitochondrial reduction of MTT to purple Formazan.	27
Figure 3.9. Gel and membrane preparation for electrophoretic transfer.	32
Figure 4.1. The effect of increasing CS:TPP mass ratios on the size of chitosan nanoparticles.....	34
Figure 4.2. The effect of increasing pH values on the size of chitosan nanoparticles....	36
Figure 4.3. Typical topographic Height Sensor image of particles in suspension obtained by atomic force microscopy (AFM).....	39
Figure 4.4. Binding efficiency between chitosan and pDNA at different CS:pDNA ratios by agarose gel retardation assay for 0 h, 24 h and 48 h.....	39
Figure 4.5. Transfection efficiency of CNs-pDNA formulations at different ration of 500:1, 300:1 and 100:1 after 96 h of transfection.....	40
Figure 4.6. Typical kindling red fluorescent protein (KFP) expression in HeLa cell line with 1% and 0.1% CNs-pDNA	41

Figure 4.7. Typical kindling red fluorescent protein (KFP) expression in MDA-MB-231 cell line with 1% and 0.1% CNs-pDNA.....	42
Figure 4.8. Typical kindling red fluorescent protein (KFP) expression in THP-1 cell line with 1% and 0.1% CNs-pDNA	43
Figure 4.9. Metabolically active HeLa cells following exposure to CNs-pDNA for 24h, 48h and 72h treatment with different concentration with the ratio of 500:1, 300:1, 100:1.....	45
Figure 4.10. Metabolically active MDA-MB-231 cells following exposure to CNs-pDNA for 24h, 48h and 72h treatment with different concentration with the ratio of 500:1, 300:1, 100:1	46
Figure 4.11. Metabolically active THP-1 cells following exposure to CNs-pDNA for 24h, 48h and 72h treatment with different concentration with the ratio of 500:1, 300:1, 100:1 and ratios of CNs-pDNA.	47
Figure 4.12. (A) Changes in the cell cycle profile due to the 72 h treatment with 1% (500:1) CNs-pDNA. (B) Changes in the DNA fragmentation profile due to the 72 h treatment with 1% (500:1) CNs-pDNA.....	48
Figure 4.13. CNs-pDNA-mediated reduction in generation of total ROS.....	50
Figure 4.14. (A) Typical micrographs of SA- β -gal positive HeLa cells (B) CNs-pDNA-induced premature senescence in HeLa cells.....	51
Figure 4.15. (A) Typical micrographs of SA- β -gal positive MDA-MB-231 cells (B) CNs-pDNA-induced premature senescence in MDA-MB-231 cells ...	52
Figure 4.16. (A) Typical micrographs of SA- β -gal positive THP-1 cells (B) CNs-pDNA-induced premature senescence in THP-1 cells.....	53
Figure 4.17. Effect of 1% 500:1 CNs-pDNA on protein expression profiles.....	54
Figure 4.18. Due to the higher availability, cells belonging to the blood system are more susceptible to CNs-pDNA treatment that these derived from solid tissues.....	55

LIST OF TABLES

<u>Table</u>	<u>Page</u>
Table 3.1. General Properties of pKindling-Red-Mito Vector.	16
Table 4.1. Size, zeta potential and polydispersity index (P.I.) of the chitosan nanoparticles for different ratio of CS:TPP.....	35
Table 4.2. Size, zeta potential and polydispersity index (P.I.) of the chitosan nanoparticles for different pH values.	36
Table 4.3. Physical and chemical characteristics of different CNs-pDNA formulation (500:1, 300:1 and 100:1)	38

LIST OF ABBREVIATIONS

AFM	Atomic force microscopy
BCA	Bicinchoninic Acid
BSA	Bovine Serum Albumin
CNs	Chitosan Nanoparticles
CNs-pDNA	plasmid DNA loaded chitosan nanoparticles
DD	Degree of deacetylation
DLS	Dynamic light scattering
DMEM	Dulbecco's Modified Eagle's Medium
EE	Encapsulation efficiency
EMA	European Medicines Agency
FBS	Fetal Bovine Albumin
FDA	Food and Drug Administration
GFP	Green Fluorescent Protein
HeLa	Human cervical cancer cell line
IC ₅₀	Half maximal inhibitory concentration
KFP	Kindling Red Fluorescent Protein
LDV	Laser Doppler Velocimetry
LMWC	Low molecular weight chitosan
MDA-MB-231	Breast cancer cell line
MW	Molecular weight
Ns	Nanoparticles
PBS	Phosphate buffered saline
PI	Polydispersity index
RPMI-1640	Roswell Park Memorial Institute Medium
SA- β -gal	Senescence-associated β -galactosidase activity
SD	Standard deviation
THP-1	Peripheral blood cell line
TPP	Pentasodium tripolyphosphate
ζ / ZP	Zeta potential

CHAPTER 1

INTRODUCTION

Gene therapy is one of the most promising strategies for treatment of various diseases such as cancer and inflammatory, neurological, cardiovascular or metabolic disorders (Ragelle et al. 2014; Ibraheem, Elaissari, and Fessi 2014). Simultaneously, the choice of a good transfection agent for delivery of nucleic acids is critical for each gene transfer procedure, however most commercially available transfection agents have still some limitations (Perez-Martinez et al. 2011). More recently, in gene delivery, viral vectors are still used due to the high transfection efficiency compared to non-viral gene delivery systems. However; the clinical applications of the viral vectors are limited by toxicity issues such as immunogenicity and mutagenicity. Taking into account safety considerations, non-viral vectors are thought to be a more promising nucleic acid carrier compared to viral vectors (Ishii, Okahata, and Sato 2001b).

Among non-viral vectors, chitosan (CS) is one of the most commonly studied polymer since its positive charge under slightly acidic conditions allow its interaction with the nucleic acid and thus formulation of complexes of nanoparticles (Ragelle et al. 2014). On the other side, it is known that many biological effects caused by nanoparticles depend on their size, shape, used dose, behavior of nanoparticles in environment (i.e., whether or not their aggregation occurs) and cell type (i.e., suspended versus adherent cell types or healthy versus cancer cell types) (Fu et al. 2014; Mytych, Pacyk, et al. 2015; Mytych, Lewinska, et al. 2015). It has been already shown that plasmid DNA loaded chitosan nanoparticles (CNs-pDNA) did not cause any cytotoxicity to macrophages (which differentiate from monocytes). Furthermore, CNs-pDNA did not induce secretion of proinflammatory cytokines and the triggered release of metalloproteinases linked to NPs degradation, not inflammatory reactions (Chellat et al. 2005). Despite these promising results, potential side effects including cytostatic or cytotoxic effects caused by biodegradable nanomaterials like CNs or/and type of used expression vector system on different cell types are only poorly understood. Previously, some researchers reported that GFP transduction might affect the cytophysiology of targeted cell. For example, it is widely accepted that tagged chromosome proteins may

affect the motion of chromosomes. In general, GFP is considered nontoxic both in *in vitro* and *in vivo* systems. However, there are some reports showing side effects of GFP in *in vitro* and *in vivo* studies, although details of molecular mechanism of these interactions still remain unclear (Liu et al. 1999; Agbulut et al. 2006; Huang et al. 2000; Agbulut et al. 2007; Baens et al. 2006). More recently, it has been shown that Ku80 attenuates cytotoxicity induced by green fluorescent protein transduction independently of non-homologous end joining (Koike, Yutoku, and Koike 2013).

Moreover, the application of biodegradable nanomaterials as nucleic acid delivery systems for living organisms including humans raises also other important questions about the impact of CNs on efficiency of pDNA condensation. Matsumoto et al., (2009) showed the differences in the transcriptional activity of pDNAs transfected into cells using either cationic lipids or cationic polymers (Matsumoto et al. 2009).

Therefore, in this study, we aimed to use the ionic gelation method for the encapsulation of pKindlig-Red-Mito vector into chitosan nanoparticles and to evaluate their potential as safe-nanocarriers on different cell line models derived from human solid tissues cancers (HeLa and MDA-MB-231) and monocytes (derived from peripheral blood cancer – THP-1).

This thesis includes five chapters. Chapter 1 aims to present a brief introductory background to the research subject. Previous relevant studies about the history of gene therapy which is the field of related with chitosan-plasmid DNA nanoparticles, the chemistry (synthesis properties) and application of chitosan as a biomaterial are reviewed in Chapter 2. The experimental part (Chapter 3) of the thesis aims to provide a comprehensive analysis concerning this study. It also elaborates the materials devices and methods that were used in particle preparation and *in vitro* applications. In Chapter 4, results are presented and discussed with regard to particles' physical-chemical properties, cellular uptake and transfection efficiency, cytotoxic and cytostatic properties. Finally, in Chapter 6, the main results and the conclusions of the study are summarized.

CHAPTER 2

LITERATURE REVIEW

2.1. Gene Therapy

The European Medicines Agency (EMA) defines the gene therapy medicinal product: “a biological medicinal product that contains an active substance, which contains or consists of a recombinant nucleic acid used in or administered to human beings with a view of regulating, replacing, adding or deleting a genetic sequence, as well as if its therapeutic, prophylactic or diagnostic effect relates to the recombinant nucleic acid sequence it contains, or to the products of genetic expression of this sequence”(European Medicines Agency 2010). Basically gene therapy is termed as the transfer of genetic material into the cells of a patient to produce a therapeutic benefit (Anderson 1992; Baltimore 1988; Mizutani et al. 1995; Saraswat et al. 2009).

Since the discovery of DNA, the potential of treating or preventing disease by modifying the expression of one’s genes has considered. During 1960’s and 1970’s, recombinant DNA researches proved the possibility of genetic material transfer into mammalian cells for the purpose of therapy (Wirth, Parker, and Ylä-Herttuala 2013). Over the past decades, many inheritable or acquired human diseases can be treated by silencing gene expression, replacing genes and supplying the missing genes (Ibraheem, Elaissari, and Fessi 2014). Up to year 2015, approximately 2200 clinical trials in gene therapy approved worldwide have been applied and are still ongoing (Wiley 2015). However both the Food & Drug Administration (FDA), and the EMA have not approved any human gene therapy product for commercial use so far (Thomas and Seppo 2011).

In this context, currently gene therapy is considered as one of the most promising strategies for treatment of various diseases such as cancer and inflammatory, neurological, cardiovascular or metabolic disorders (Ragelle et al. 2014; Ibraheem, Elaissari, and Fessi 2014; Mao, Sun, and Kissel 2010). The success of application is largely dependent on the development of a vector or vehicle that can selectively and

efficiently deliver a gene to target cells with minimal toxicity (Mao, Sun, and Kissel 2010; Dewey et al. 1999) .

2.1.1. Gene Transfer Methods

Various delivery systems have been developed for nucleic acid delivery because it is very difficult to pass through plasma membrane since their physicochemical properties such as size, surface charge and hydrophilicity (Mannell et al.; Iwashita et al. 2012; Siu et al. 2012; Jin et al. 2014) . Recently, gene delivery systems possess two of groups as viral and non-viral (chemical, mechanical or physical methods) methods (Jin et al. 2014). Viral gene delivery is associated with transporting nucleic acids by viral vectors such as adenoviruses vectors, adeno-associated vectors, retroviral vectors, lentivirus vectors, herpes simplex virus vectors and poxvirus vectors. Non- viral gene delivery systems contain two major groups as mechanical or physical methods and chemical methods as shown in Figure 2.1.

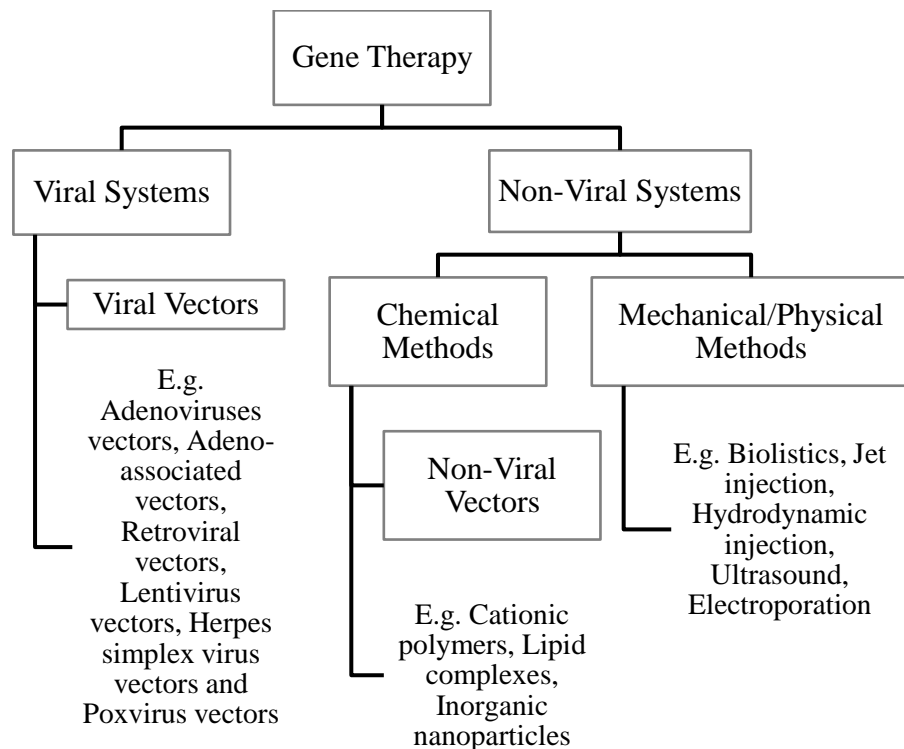


Figure 2.1. The basic of gene delivery systems for gene therapy (Source: Zhang and Godbey 2006; Yamamoto and Tabata 2006; Niidome and Huang 2002; Jin et al. 2014).

Each vector type exhibits its own specific characteristics. For example, viral vectors present higher transfection efficiencies *in vivo* and *immunozation* (Lim et al. 2006).

2.1.2. Plasmid DNA Based Therapeutics

Plasmids are high molecular weight, double stranded DNA constructs containing transgenes, which encode specific proteins. According to the mechanism of action of pDNA, plasmid DNA molecules should enter the nucleus after entering the cytoplasm. This affects directly the efficiency. Other than the disease treatment, pDNA molecules can be used as vaccines for the immune system (Scholz and Wagner 2012; Johnston, Talaat, and McGuire 2002). During early investigations, the plasmid based therapy is used to cure inheritable disorders caused by a single gene defect. In 1990, a treatment of adenosine deaminase deficiency was started and this was the first federally approved human gene therapy protocol (Johnston, Talaat, and McGuire 2002).

Taniyama et al., showed that DNA based gene therapy is used especially for cardiovascular disease (Taniyama et al. 2012). Taniyama reported that, plasmid DNA based gene transfer is safe but its efficiency is low. DNA based vaccines are becoming attractive recently. According to Ferraro, there are pDNA based vaccines which are approved for use in veterinary practice of canine melanoma, West Nile virus, fish hematopoietic necrosis virus and swine growth hormone-releasing hormone (Ferraro et al. 2011). MacGregor, R.R. et al.(1998), investigated results of immune response in 15 HIV infected patients subjected to a dna based vaccine containing HIV-1 (MacGregor et al. 1998).

2.2. Chitosan

Chitosan is one of the most abundant biodegradable polysaccharide on Earth (Wnek and Bowlin 2004). In this regard, chitosan is used in various fields and numerous applications due to their suitable characteristics such as good biocompatibility, biodegradability, antimicrobial activity and chelating abilities.

Although chitin is a structural mucopolysaccharide in a wide range of species such as arthropods, cephalopods, algae and most fungi, chitosan has only been found in the cell walls of certain fungal species (Dumitriu 2004; Teoh 2004; Dumitriu 2001).

In 1811, Henri Braconnot discovered ‘chitin (fungine)’ when he was studying on mushrooms (Dumitriu 2001). The term “chitin” is derived from the Greek word “chiton” signifying nail coat (Shahidi and Abuzaytoun 2005). Chitosan was discovered by C. Rouget and initially named as “modified chitin” when he studied chitin with boiling and concentrated potassium hydroxide in 1859 (Stephen 1995). Currently, chitin and chitosan possess a wide range of application areas include agriculture, cosmetics, dietetics, pharmacology, gene therapy, and biomaterials (Dumitriu 2001; Shahidi and Abuzaytoun 2005).

2.2.1. Chemical Structure of Chitin and Chitosan

Chitin and chitosan are belong to the family of glycosaminoglycans (GAGs) which is a subcategory of polysaccharides. Chitosan is a linear, natural copolymer of β -(1-4)-linked D-glucosamine and N-acetyl-D-glucosamine (NAG) units which are protonated in slightly acidic conditions so as positively charged in most physiological fluids (Dash et al. 2011).

Chitin and chitosan occur in three different polymorphic forms, namely α -, β - and γ -chitin depending on the source organism (Borchard 2001; Jang et al. 2004). Alpha-chitin is presents in arthropods, fungi or cysts of *Entamoeba* associated with an antiparallel chain packing at specific intramolecular and intermolecular hydrogen bonding. Beta-chitin is basically found in the pen of the Loligo squid, is identified with the parallel arrangement of chitin molecules that leads to weak intermolecular forces (Jang et al. 2004) and higher reactivity than α -chitin . Gamma-chitin is found in cocoon fibers of the Ptinus beetle and in the stomach of Loligo squid (Allin 2004; Jang et al. 2004; Borchard 2001). In its structure, two layered is present in a parallel arrangement at which intercalated by a layer in antiparallel packing (Roberts 1992). The selection of the source for chitosan production is important as so chitosan derived from β -chitin shows higher reactivity than α -chitin (Kurita et al. 1994).

Chitosan is mainly produced by the deacetylation of chitin in highly concentrated alkali conditions. The treatment of sodium or potassium hydroxide (40-

50%), at temperatures of 100-150°C for periods of 1-5 h under heterogeneous conditions results results in approximately 70% deacetylated chitosan (Borchard 2001; Kurita 2006; Ravi Kumar 2000). The molecular weight of the chitosan decreases with repeating the procedure.

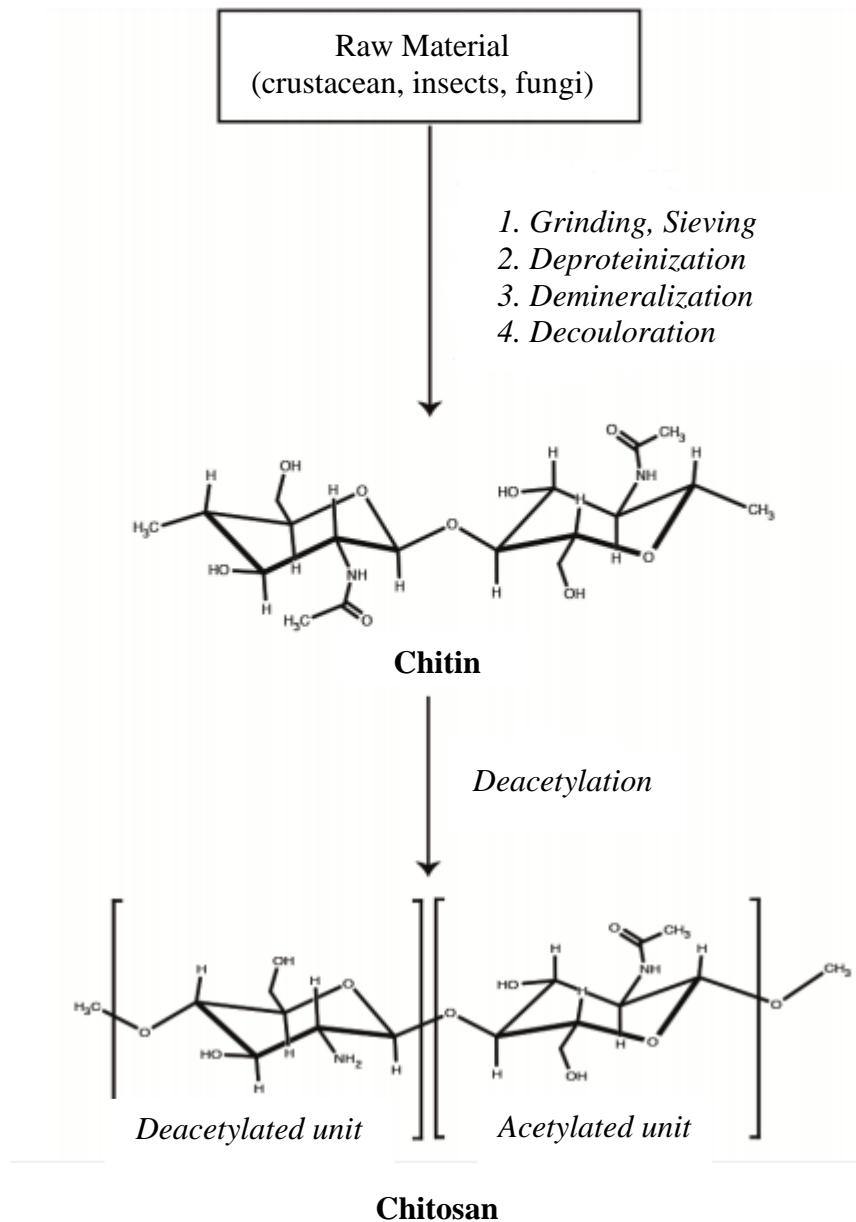


Figure 2.2. Schematic representation of Chitosan manufacturing process from Chitin (Source: Agirre et al. 2014).

In addition, deacetylation degree (DD) is one of the ways to separate the structure of chitin from chitosan. Commonly a majority of D-glucosamine units in the material refers the the substance is chitosan (Teoh 2004).

On the other side, chitosan basically has three reactive functional groups including a primary amino group at the C-2 position, a primary and secondary hydroxyl group at the C-3 and C-6 positions (Pillai, Paul, and Sharma 2009; Lv et al. 2009). Chitosan and its functional groups are represented in Figure 2.2.

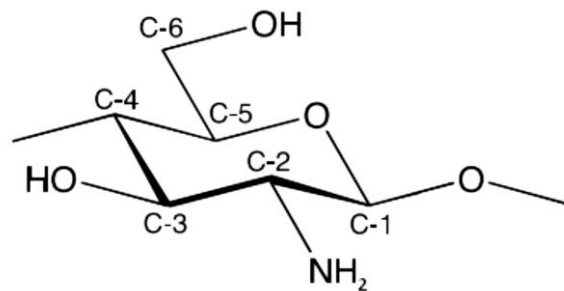


Figure 2.3. Functional groups of chitosan: primary amino group at positions C-2, primary hydroxyl group at positions C-3 and secondary hydroxyl group at positions C-6 (Source: Kurita 2006).

Chitosan is considered as potential carrier for nucleic acid delivery depending on its cationic charge due to the free primary amine groups in component units. The primary amines of chitosan become positively charge under acidic condition at pH under the pKa value of chitosan (~ 6.5) which permits the nucleic acids to form polyplex with chitosan (Mao, Sun, and Kissel 2010).

2.2.2. Biological Properties of Chitosan

Chitosan possesses not only biocompatibility and biodegradability properties but also antimicrobial, antitumor and antiviral activity that becomes chitosan attractive material for biomedical and pharmaceutical application (Ravi Kumar 2000; Dash et al. 2011; Pillai, Paul, and Sharma 2009; Rojanarata et al. 2008). The physicochemical nature of chitosan, influences strongly the biomedical activity (Kumirska et al. 2011).

Illium and colleges observed that the lethal dose (LD₅₀) for oral administration of chitosan is 16 g/kg for rabbits and 10 g/kg for mice (Illum 1998). Moreover, due to the cationic nature chitosan can easily interacts with negatively charged erythrocytes in

blood stream. It was reported that this cationic nature of chitosan cause also hemorrhagic pneumonia in dogs at the high doses of 200 mg/kg (Illum 1998).

On the other hand, it has been already shown that chitosan nanoparticles and plasmid DNA loaded chitosan nanoparticles (CNs-pDNA) did not cause any cytotoxicity to macrophages (which differentiate from monocytes). Although these promising results, potential side effects including cytostatic or cytotoxic effects caused by biodegradable nanomaterials like CNs or/and type of used expression vector system on different cell types are only poorly understood. More knowledge is needed about the cytotoxicity and cytostatic effects of non-viral vectors.

2.3. Chitosan as a Non-viral Vector

Due to the physicochemical properties, cationic polymers are attractive alternative for nucleic acid transport as nonviral delivery systems (Kean and Thanou 2010; Tong et al. 2009). The first chitosan was used as a non-viral carrier for pDNA delivery in 1995 by Mumper et al. In 1998, Mumper and his friends also used chitosan-pDNA nanoparticles for *in vivo* transfection and showed the promising potential of chitosan as non-viral vector (MacLaughlin et al. 1998). Chitosan usage in nucleic acid delivery is increasing in the recent years.

Although chitosan promising candidate as non-viral vector, it shows low stability, buffering capacity and cell specificity.

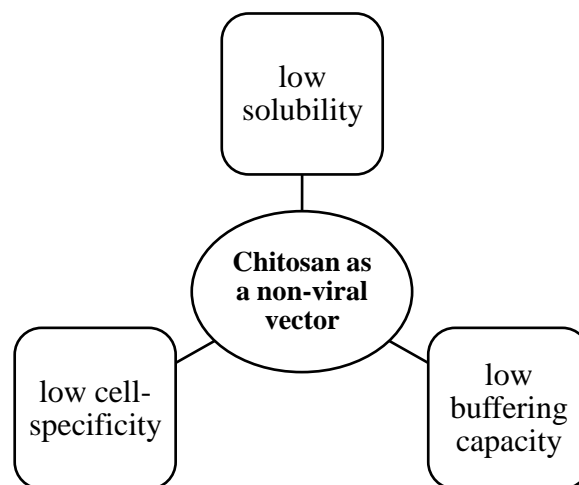


Figure 2.2. The drawbacks of chitosan as non-viral vector.

The stability and transfection efficiency of polyplexes associated with chitosan structural variables. In this part, the factors that affect the quality of the transfection will be discussed.

The degree of deacetylation (DD) and molecular weight (MW) are initially two factors that determine the physicochemical properties of chitosan, and consequently significantly affects the transfection efficiency. One of these factors, the molecular weight (MW) of chitosan influences the particle size, polyplex stability, cellular uptake, release of nucleic acids from the polyplex and thus the transfection efficiency (Mao et al. 2001). According to MacLaughlin, the size of polyplex shows rise with higher MW of chitosan (MacLaughlin et al. 1998). Also it was reported that high molecular weight chitosans exhibit better DNA integrity although the release of DNA restricted due to the high stability of the complex (Huang et al. 2005). On the other hand, Liu was reported that polyplexes formed from low molecular weight chitosan were less stable due to the weak interaction between chitosan and nucleic acids (Liu et al. 2007).

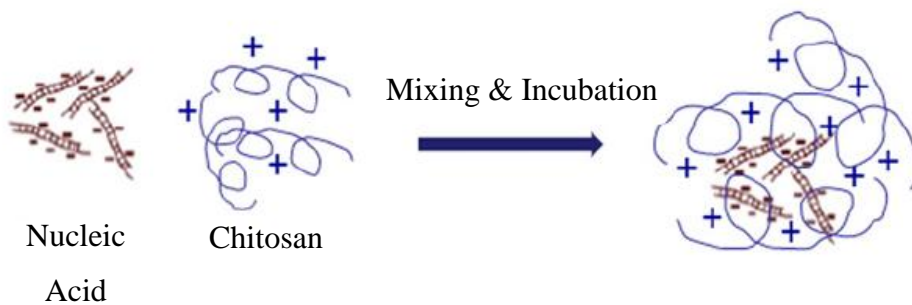
Other factor, the degree of deacetylation (DD) refers the percentage of deacetylated primary amine groups on the molecular backbone which determine the positive charge density in acidic condition (Mao, Sun, and Kissel 2010). In this context, high deacetylation (DD) causes an increased positive charge thus strong electrostatic interaction and stable polyplexes. Kiang was also reported that the degree of deacetylation should be higher than 65% to obtain stable polyplex with plasmid DNA (Kiang et al. 2004). As a summary, to obtain desirable effective polyplex, taking together appropriate MW and DD should be for lowering MW increasing DD, for lowering DD increasing MW (Lavertu et al. 2006).

The formation of particles through this method occurs at a specific chitosan/nucleic acid ratio. This N/P ratio associates with the ratio between the nitrogen (N) of chitosan per the phosphate (P) of DNA (Mao, Sun, and Kissel 2010). The N/P ratio is also important for the particle net surface charge which affects the interaction with negatively charged cell membrane, thus the transfection efficiency. The polyplex N/P ratio must be high enough to release the nucleic acid inside the cell efficiently. If the N/P ratio is too low, polyplex will be unstable physically. If the N/P ratio is too high, nucleic acid will not release efficiently to the cell. Both two conditions show reduced transfection. Ishii and colleagues also demonstrated that the transfection efficiency of chitosan/DNA complexes increased at the ration of 3:1 and 5:1 and decreased at 10:1 and 20:1 on SOJ cells (Ishii, Okahata, and Sato 2001a).

On the other side, the transfection efficiency of chitosan-based non viral vectors highly depends on the pH of the culture medium. At the pH of 5.5-5.7, the amine groups of chitosan protonated ~ 90% (Mao et al. 2001) and at the neutral or basic pH the degree of protonation is reduced thus particles aggregated in medium. Previously studies indicated that optimal transfection efficiency can be obtained at the pH range of 6.5-7.0 (Sato, Ishii, and Okahata 2001). Liu et al. also reported that lower pH causes poor transfection efficiency (below pH 6.5).

Chitosan-based nucleic acid nanoparticles can be prepared by different methods such as complex coacervation (Mao et al. 2001), ionic gelation (Katas and Alpar 2006; Csaba, Koping-Hoggard, and Alonso 2009).

Simple Complexation



Ionic Gelation

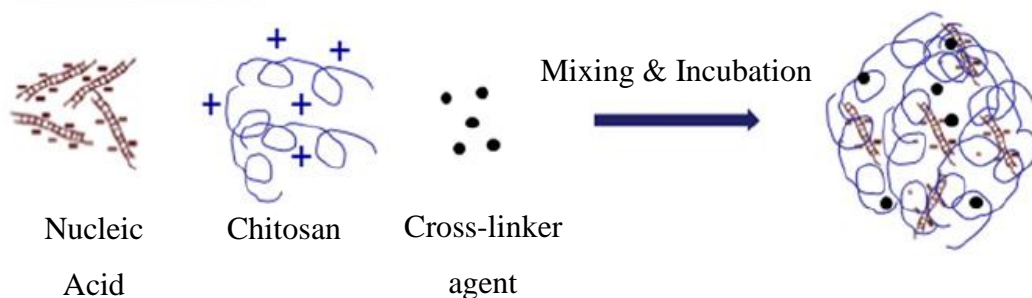


Figure 2.3. Schematic representation of the main methods for formulating chitosan-based nanoparticles for nucleic acid delivery (Source: Ragelle, Vandermeulen, and Preat 2013).

Katas et al. reported that chitosan-siRNA nanoparticles formulated by simple complexation showed less than 20% gene silencing due to the weak interactions between nucleic acids and chitosan. Cross-linker agents supply higher stability in the formation of nanoparticles (Ravina et al. 2010; Katas and Alpar 2006). Katas et al. showed that chitosan-siRNA nanoparticles formulated by ionic gelation method have

82% luciferase silencing efficiency on CHO K1 cells (Katas and Alpar 2006). Also Rojanarata and colleagues obtained 70% GFP silencing efficiency on HepG2 cells by CS-TPP/siRNA (Rojanarata et al. 2008).

2.4. Barriers for Cellular Delivery of Non-viral Vectors

Although the significant potential of nucleic acid based therapeutics, a major problem is to develop safe and effective delivery systems to transport nucleic acid to the site of action in the cells of target tissues. The self-defense mechanism of human body against to the foreign materials and pathogens causes several delivery barriers. In this section, the major barriers to nucleic acid delivery will be discussed.

2.4.1. Extracellular Barriers

The extracellular barriers for cellular delivery of non-viral vectors associated with the route of administration such as intranasal, intraocular, topical, oral and systemic intravenous injection (Miyata, Nishiyama, and Kataoka 2012). Once nucleic acids were injected into the blood stream, the barriers including reticuloendothelial system (RES), nuclease degradation and renal clearance system encountered them (Whitehead, Langer, and Anderson 2009; Wang et al. 2010).

In blood circulation, the presence of nucleases is one of the most important barrier that degrades DNA and thus to design powerful vector for the protection of nucleic acid from degradation is essential. Another barrier is reticuloendothelial system (RES) which occurs phagocytic cells such as monocytes in tissue macrophages and blood stream. Mainly function of the reticuloendothelial system (RES) is to kill the foreign matters and to remove by macrophages (Mosser and Edwards 2008). With the surface modification of vectors, such as polyethylene glycol (PEG) (Bailon and Won 2009) and poly[N-(2-hydroxypropyl)methacrylamide] (pHPMA) (Lu 2010), they can escape from protein binding and macrophage internalization.

On the other hand, renal clearance system is also important for the delivery of vectors in human body. Kidneys remove waste products of metabolism by glomerular filtration. Here the size of molecule is critical parameters for renal excretion. Molecules under ~40 kDa can be easily secreted though renal clearance (Seymour et al. 1987;

Bailon et al. 2001). According to Nishina et al, the conjugation of nucleic acids with polymers or lipids can be reduce the renal excretion (Nishina et al. 2008).

2.4.2. Intracellular Barriers

After the nucleic acid loaded particles reached to the target cells, there are several barriers that must be considered such as internalization by cell membrane, endosomal escape and then reach to the nucleus (Parker et al. 2003). Once the particles reach to the target cells, they are bound to the cell membrane. Due to the negatively charged cell membrane, electrostatic interactions occur with positively charged vectors. Naked nucleic acids cannot enter cells successfully because of the size and negative charge. Endocytosis is the most common pathway of internalization divided into types: clathrin-mediated endocytosis (CME), caveolae-mediated endocytosis (CvME), clathrin- and caveolin- independent endocytosis, phagocytosis and macropinocytosis (Khalil et al. 2006). In this context, internalization mechanisms are strongly dependent on the physical and mechanical parameters of particles and the cell type (Hillaireau and Couvreur 2009).

After the internalization of nucleic acid to the cell, the other important barrier for nucleic acid delivery is endosomal trapping. For example pDNA need to release successfully to the cytoplasm and reach to the nucleus for transcription. Unless the vector escapes successfully from the endosome, nucleic acid will be degraded by lysosomes (Varkouhi et al. 2011). There are several mechanisms reported for the endosomal escape such as *proton-sponge effect* (Boussif et al. 1995) and *membrane fusion* (Wagner 1999). The pH-buffering effect or proton sponge affect is depends on the buffering capacity of delivery system. For example, chitosan, polyethylenimine (PEI) and polyamidoamine (PAMAM) lead to alteration to the surrounding environment resulting in osmotic swelling and endosome breaking with their pH and buffering capacity (Boussif et al. 1995). As a whole, delivery materials which possess high buffering capacity at endosomal pH or conjugation of disturbing peptide and pH-responsive polymers should be studied for efficient gene delivery (Agirre et al. 2014)

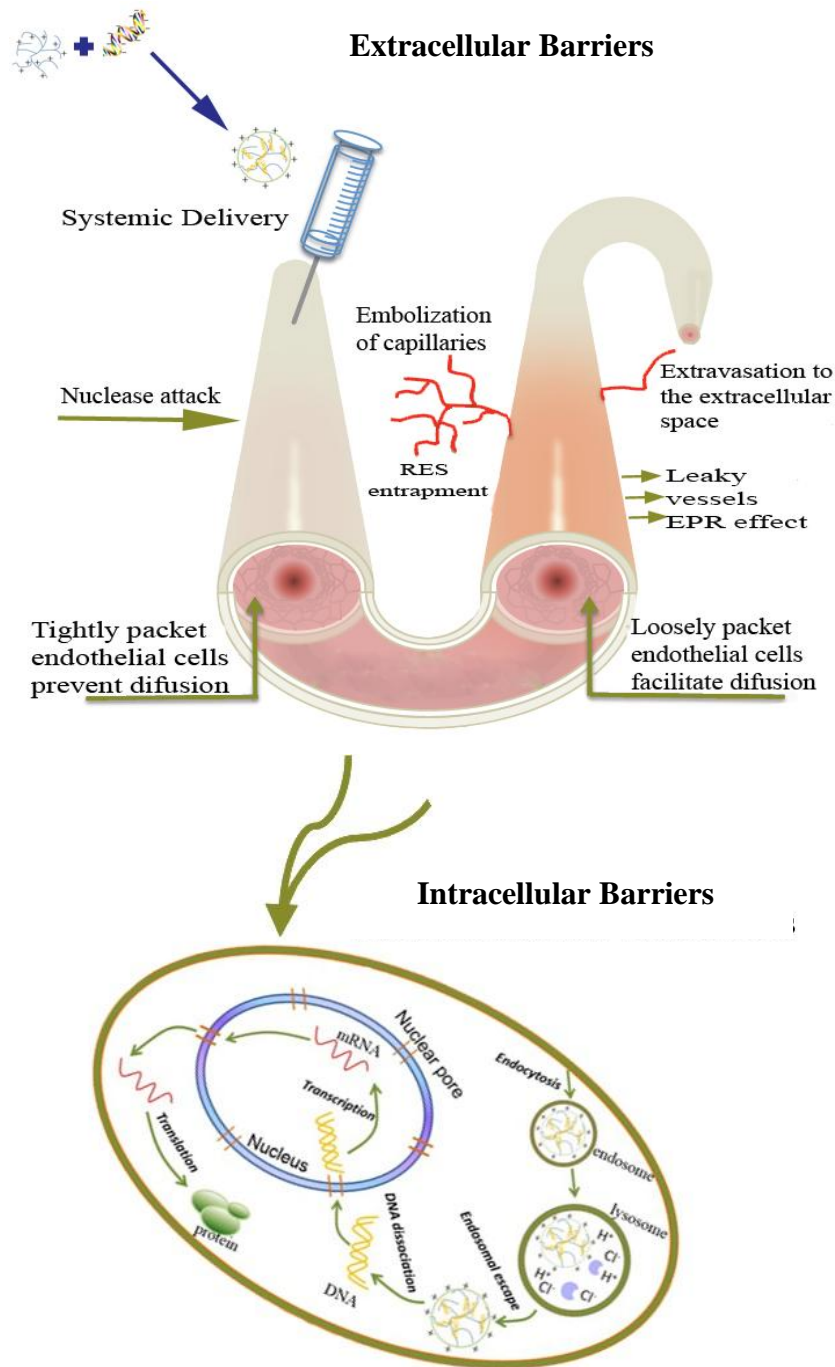


Figure 2.4. Mainly extra- and intracellular barriers for non-viral gene delivery (Source: McCrudden 2013; Jin 2014)

2.5. Cytotoxicity and Nanomaterials

Toxicology basically means potentially harmful effects of chemicals and materials to the living organism and the environment. Principle of toxicology associated with Paracelsus who is attributed with the expression of the classic toxicology "All things are poison and nothing is without poison; only the dose makes a thing not a

poison." (Borzelleca 2000; Elsaesser and Howard 2012). In this context the nanotoxicology refers to the study of the potentially harmful effects of nanomaterials, in particular nanoparticles (NPs) (Donaldson et al. 2004).

Nanotechnology is the study and widely used in extremely areas such as cosmetics, sunscreens, textiles and sport items and veterinary medicines. (Bottero et al. 2015). All scientists agree that development of the nanotechnology is important for all humanity and currently discussing the future effects. New materials can be create with nanotechnology in different areas such medicine, biomaterials, energy, electronics, industry, environmental, or human health. On the other hand, it helps development of the new technologies including concerns about the toxicity and also helps to solve social and economical problems in various scenarios. Besides, it should be careful to determine possible toxicity of nanotechnology derived products before widespread use (Oberdörster 2004).

Nanotechnology science provides technological solutions in many environmental problems such as pollution, climate change and clear drinking water such as nanomaterials can detect, prevent and remove pollutants (Lee, Scheufele, and Lewenstein 2005) and can design cleaner industrial process and environmentally products (Kamat and Meisel 2003).

CHAPTER 3

MATERIALS AND METHODS

3.1. Materials

Cell culture studies were performed at Dr. Maciej Wnuk's laboratory. Chemicals and solutions that are necessary in cell culture studies were obtained from Department of Biotechnology, University of Rzeszów.

Throughout this study, chitosan (CS) with average low molecular weight of (LMWC) ~120 KDa and degree of acetylation (DD) of 75-85 % and was used (Sigma-Aldrich, USA). Plasmid DNA (pDNA) encoding red fluorescent protein (KFP) were purchased from Evrogen JSC. Some important properties of pKindling-Red-Mito can be seen in Table 3.1.

Table 3.1. General Properties of pKindling-Red-Mito Vector (Source: Evrogen).

pKindling-Red-Mito Vector	
Vector Type	mammalian expression vector
Reporter	KFP-Red
Reporter codon usage	mammalian
Promoter for KFP-Red	P _{CMV IE}
Host cells	mammalian
Selection	prokaryotic-kanamycin eukaryotic-neomycin (G418)
Replication	prokaryotic - pUC ori eukaryotic - SV40 ori
Use	monitoring the movements of individual mitochondria

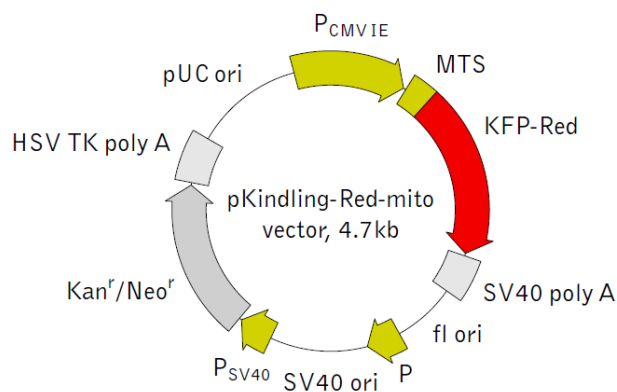


Figure 3.1. Schematic presentation of pKindling-Red-Mito Vector (Source: Evrogen).

In this study, detailed list of used chemicals, buffers, solutions and their compositions are presented as *Appendix A*, *Appendix B*, *Appendix C* *Appendix D*.

3.2. Methods

3.2.1. Preparation of Bacterial Plasmids

The plasmid pKindling-Red-Mito encoding KFP was grown in DH5 α as host strains. Kanamycin (30 μ g/ml) was used for resistance of the vector in *E. coli* hosts. The concentration of isolated plasmids in the sample was calculated at 260 nm by NanoDrop™ 2000/2000c Spectrophotometers. The absorbance ratio of A_{260}/A_{280} provided an estimate for the purity of the plasmids between 1.7-1.9.

A) Preparing Competent Cells: For the preparation of the competent cells; 30 mL of SOB broth inoculated with bacteria to be transformed from a plate and incubated overnight at 37°C under moderate agitation. The overnight culture (8 mL) added to a flask (2 L) containing 200 mL of SOB broth and incubated again at 37°C under moderate agitation until an OD550 of approximately 0.3 is reached. The culture centrifuged at 5000 rpm for 15 minutes at 4°C and discharged the supernatant thoroughly. Cold transformation buffer I (16 ml in 50 ml of initial culture) added for resuspension of the pellets by mild vortexing. After incubation for 15 minutes on ice, the cells centrifuged again at 5000 rpm

for 15 minutes at 4°C and resuspended the pellets in cold transformation buffer II (4 ml in 50 ml of initial culture). The cell suspension aliquoted into microcentrifuge tubes and stored at -80°C.

B) Transforming the cells: Frozen competent cells were thawed on ice with pre-chill polypropylene tubes. After that 20 µl of plasmid DNA were added to 300 µl of cells to the prechilled tubes and gently stirred the cells while pipetting. The tubes were rolled gently for a few minutes (on ice) and incubated the cells on ice for 40 minutes. After the cells incubated at 42°C for 45 seconds without shaking cells (Heat Shock), 1 ml of L-broth (no antibiotics) were added to each tube, and incubated cells at 37°C on a roller for 45 minutes to 1 hour to allow for plasmid expression. The cells were plate out on appropriately supplemented solid media and incubated transformants at 37°C overnight.

C) Plasmid Isolation: Plasmid DNA was isolated using the GeneJET™ Plasmid Miniprep Kit, which is based on a modified alkaline lysis procedure, followed by binding of plasmid DNA to an anion exchange resin under appropriate low salt and pH conditions, according to the manufacturer's protocol. The DNA pellet was washed two times with 70% ethanol and dissolved in 30 µl 1x TE buffer.

3.2.2. Synthesis of Chitosan Nanoparticles by Ionic Gelation Method

Chitosan nanoparticles (CNs) were synthesized following the Calvo's ionic gelation procedure (Calvo et al. 1997) with some modifications. According to this procedure, low molecular weight chitosan were used with tripolyphosphate (TPP) as a crosslinker. Chitosan was dissolved in 1% (w/v) glacial acetic acid solution. Then the pH of solution was adjusted to 5.5 with 3.0 M NaOH solution. All chitosan solutions were filtered through 0.20 µm membranes. After that chitosan nanoparticles could be formed upon adding TPP, dissolved in 1% (w/v) glacial acetic acid solution, into the solution of chitosan under magnetic stirring drop by drop. The solution was centrifuged

13500 rpm for 30 minutes. The nanoparticle suspensions were immediately subjected to further analysis and applications. The supernatant was used for further characterization analysis and the pellet was freeze-dried by lyophilization. Nanoparticles were stored at 4°C.

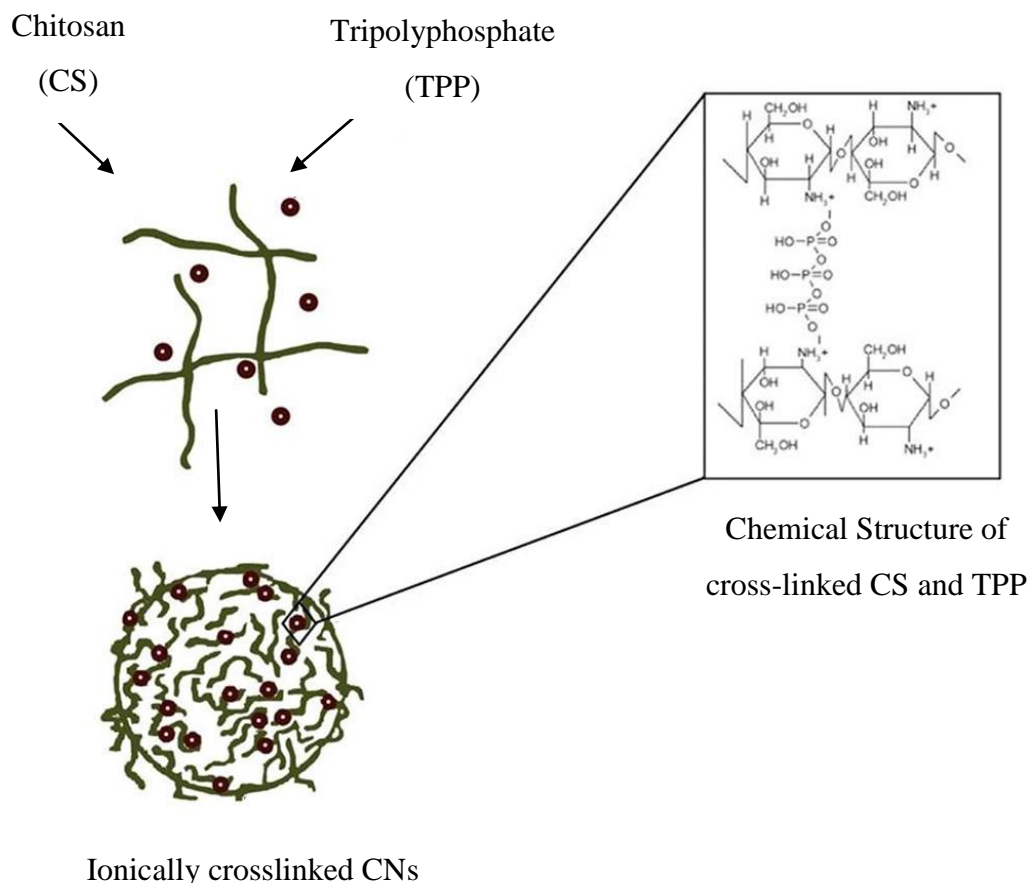


Figure 3.2. Schematic illustration of the chitosan nanoparticle formulation.

3.2.3. Synthesis of Chitosan-pDNA Nanoparticles (CNs-pDNA)

For the encapsulation, pDNA was added into the TPP solution prior to nanoparticle formation. While TPP/pDNA were dissolved in nuclease-free water, chitosan was dissolved in 1% (v/v) glacial acetic acid at different concentration in order to obtain CS:pDNA ratios 500:1, 300:1 and 100:1 at a constant pDNA concentration of 10 $\mu\text{g}/\text{ml}$. Nanoparticles could be formed upon drop wise addition of a fixed volume of TPP/pDNA solution to a fixed volume of chitosan solution under magnetic stirring.

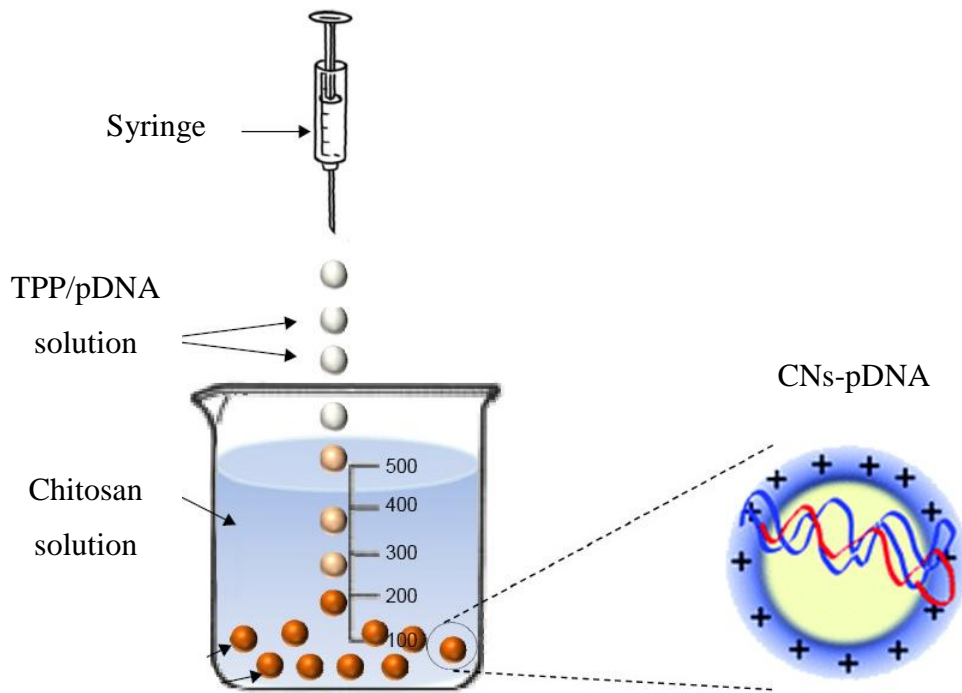


Figure 3.3. Schematic illustration of the chitosan-plasmid DNA nanoparticle (CNs-pDNA) formulation.

3.2.4. Techniques for Characterization of CNs-pDNA Particles

3.2.4.1. Dynamic Light Scattering (DLS) and Laser Doppler Velocimetry (LDV)

Dynamic light scattering (DLS) or photon correlation spectroscopy (PCS) is used for the determination of the size distribution of small sized particles in solution. A dispersed particle in a liquid medium is undergo Brownian motion which is faster with smaller particles and slower with larger particles. Illuminating the particles with laser light causes fluctuation related to individual particle size. Thus by measuring this scattering intensity fluctuation (Figure 3.4) by pinhole type photon method, the size distribution profile of particles could be obtained.

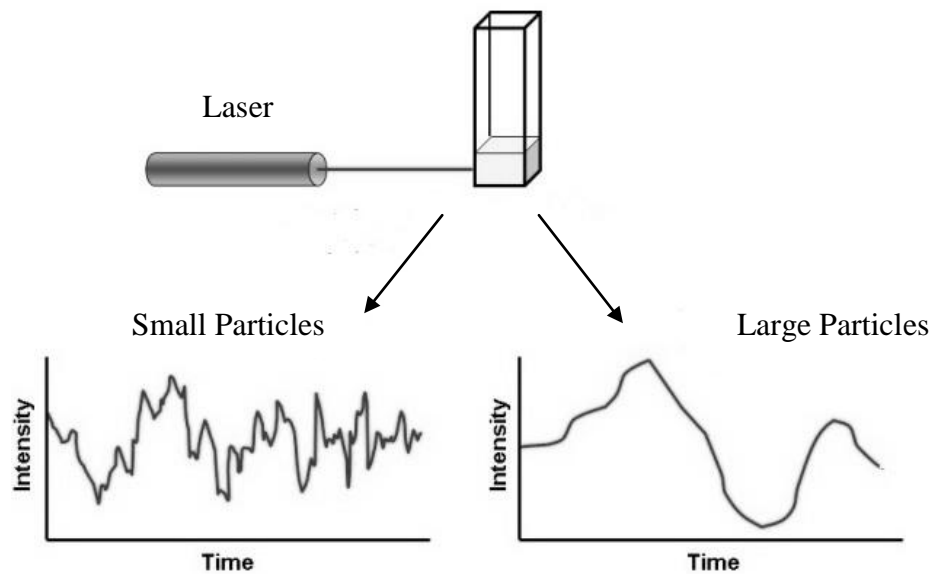


Figure 3.4. Smaller particles cause the intensity to fluctuate more rapidly than large particles in DLS measurements (Source: Malvern Instruments).

Laser doppler velocimetry (LDV) is a technique used to measure the zeta potential of particles. The knowledge of zeta potential values of the particles is important for the optimising the formulation. Especially, when chitosan nanoparticles were considered, the zeta potential measurements can be used to determine particle stability in biological systems (Lee, Powers, and Baney 2004).

All particles in suspension have a positive or negative electrostatic charge with a potential between their surfaces. When an electrical field is applied a solution, charged particles migrate in oppositely charged directions. At the same time this charged particles posses two layers on their surfaces as stern layer (inner region) and diffusing layer (outer region). As shown in Figure 3.5, stern layer consist strongly bounded ions on the surface whereas diffusing exists minimal binding force inner region. During the electrophoretic mobility, the stern layer moves whereas the diffusing layer not. There is a relative boundary between two layers called as *slipping plane* or *zeta potential*.

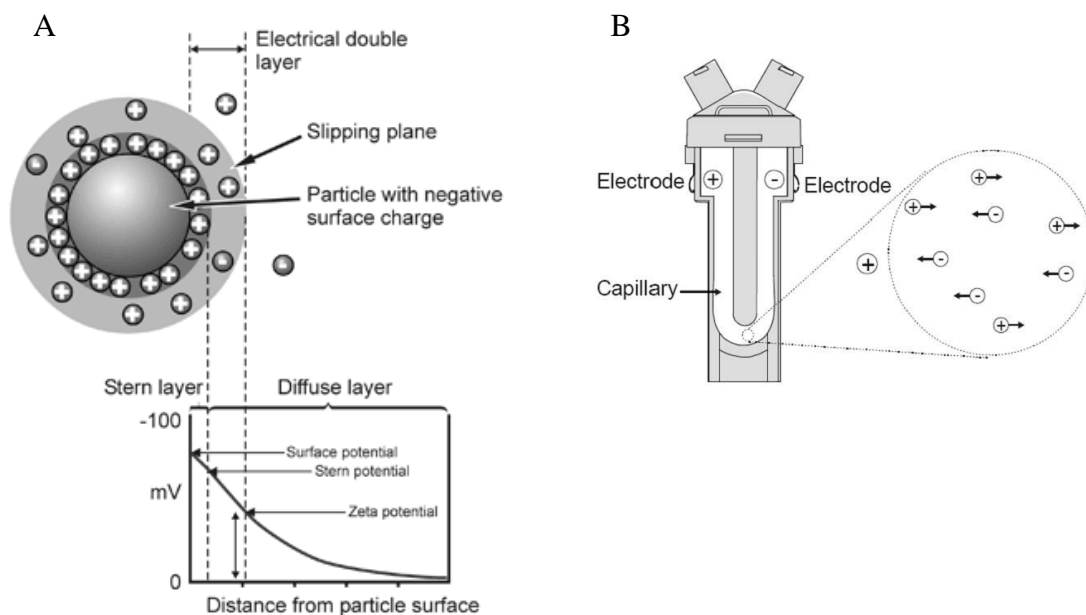


Figure 3.5. **(A)** Representation of the relation between surface charge and zeta potential value. **(B)** Principles of LDV in measuring the zeta potential (Source: Malvern Instruments).

In this project, CNS-pDNA were characterized using Zetasizer Nano ZS (Malvern Instruments Ltd, UK) for determination of mean particle diameter (Z-Average), polydispersion index (P.I.) and zeta potential values. Particle size measurements were performed at an angle of 173° when the samples in disposable cuvettes. Each measurement was performed triplicate at a temperature of 25°C in ultrapure water. After characterization of the particles, all preparations were stored at 4°C to avoid pDNA denaturation and complex dissociation.

3.2.4.2. Atomic Force Microscopy (AFM)

Atomic force microscopy is functional and versatile microscopy technology for nano-sized samples. The basic principle of AFM is based on the mapping a topographic image of the sample. During the process, the tip which is the key piece of the AFM interacts and scans the surface of sample.

When the tip is near to the analyzed surface, it undergoes attractive or repulsive forces. The cantilever, on which the tip is located, is deflected. An optical amplification system measures the tip movements.

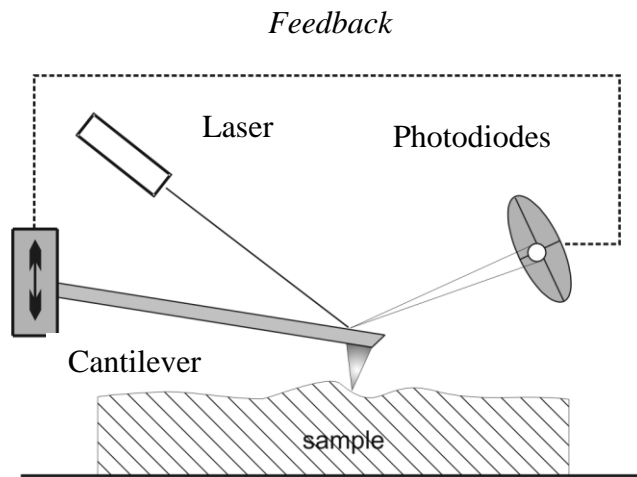


Figure 3.6. Basic principles of Atomic Force Microscopy
(Source: Saraee and Korayem 2015).

For the morphological characterization of particles, atomic force microscopy (AFM) was used. All the AFM samples have been deposited on freshly cleaved muscovite mica, incubated for 10min, and then rinsed with ultrapure water, gently flushed with a stream of nitrogen for drying. The Height Sensor and Peak Force Error AFM images were analyzed with Nanoscope Analysis software (v. 1.40 Bruker Corporation, Germany). Mean and zeta potential of the nanoparticles were determined by (Malvern Instruments Ltd, UK).

3.2.5. Determination of pDNA Encapsulation Efficiency

To determine the amount of plasmid DNA encapsulated in the chitosan nanoparticles, the difference between the total amount of pDNA and the amount of non-entrapped pDNA remaining in the supernatant after centrifugation was calculated. For this purpose, the pellet and supernatant were spectrophotometrically analyzed at 260 nm for pDNA concentration by NanoDrop™ 2000/2000c Spectrophotometers.

$$\text{Encapsulation Efficiency (\%)} = \frac{(A - B)}{A} \times 100$$

Where, "A" is the total amount of pDNA; "B" is the amount of non-entrapped pDNA.

3.2.6. Evaluation of CNs-pDNA Integrity

In this study, the stability of pDNA into the nanoparticles was also determined by gel electrophoresis assays. 1% agarose gel was prepared by 1 X TBE and heating the mixture up in a microwave on full power. After agarose was dissolved totally in TBE buffer, it was removed and cooled down.

To observe the stability of formulations in cell condition, the formulations incubated in growth medium containing 10% Fetal Bovine Serum (FBS) for 1 h, 24 h and 48 h at a temperature of 37 °C. During this study, each 1% agarose gel electrophoresis was performed triplicate. After electrophoresis procedure, all agarose gels were incubated for 15 minutes in Ethidium Bromide before visualization with G:BOX imaging system.

3.2.7. *In vitro* Studies

3.2.7.1. Cell Cultures

Human cervical (HeLa; ATCC), breast (MDA-MB-231; ATCC) (seeding density 3×10^3 cells/cm²) and peripheral blood (THP-1; ECACC) (seeding density 2×10^5 cells/ml) cancer cells were cultured in Dulbecco's Modified Eagle's medium (DMEM) (for HeLa and MDA-MB-231) or Roswell Park Memorial Institute medium (RPMI 1640) (for THP-1) supplemented with 10% fetal bovine serum (FBS) and an antibiotic and antimycotic mixed solution (100 U/ml penicillin, 0.1 mg/ml streptomycin and 0.25 mg/ml amphotericin B) at 37°C in a humidified atmosphere in the presence of 5% CO₂ until they reached confluence. Typically, cells were passaged by trypsinization (adherent cells) or direct dilution (suspension cells) to a seeding density. Microscope images of HeLa, MDA-MB-231 and THP-1 cells are represented in Figure 3.7.

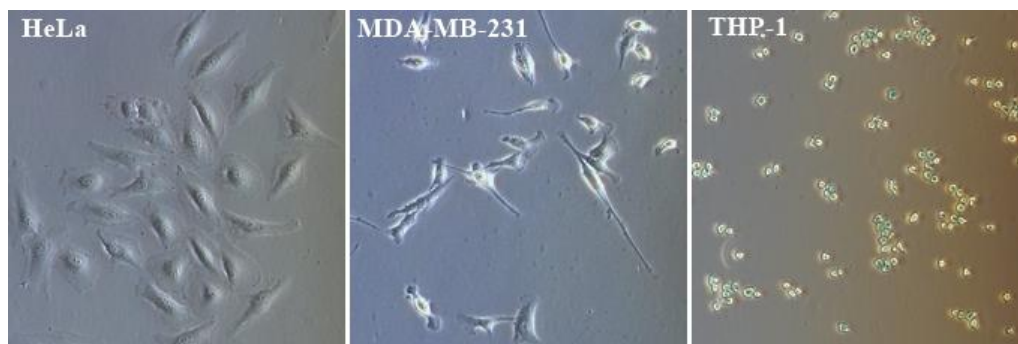


Figure 3.7. Microscope images of HeLa, MDA-MB-231 and THP-1 cell lines.

3.2.7.2. Passaging of Cell Lines

In this study, basically the cells were passaged by direct dilution (suspension cells; THP-1) and trypsinization (adherent cells; HeLa and MDA-MB-231). During the cultivation process, the cells were kept more than 10 % confluent but less than 80-90 % (log phase of growth). In order to passage adherent cells, firstly old medium was removed from tissue culture flask and the surface was washed with of Phosphate Buffering Saline (PBS). After that Trypsin/EDTA (Sigma) was added on the flask an incubated for 2-3 minutes at 5% CO₂ at 37°C. In order to inactivate the trypsin, growth medium was added by washing the flask. After collect all the cell suspension into the falcon, it was centrifuged at 800 rpm for 5 minutes at room temperature. For suspension cells the cells transferred to the falcon without trypsinization process and centrifuged at same conditon. After centrifugation, supernatant was removed from the falcon and the pellet was resuspended with 2 mL of growth medium. From this cell suspension, 100 µl of cells were transferred to an eppendorf tube for cell counting and 900 µl of trypan blue were added into the tube. After the calculation by hemocytometer, the cells were prepared at a suitable concentration (3×10^3 cells/cm² for HeLa and MDA-MB-231, 2×10^5 cm² for THP-1). Next, it was transferred into a sterile filtered tissue culture flask (25 cm², 75 cm² or 150 cm²) and completed total volume of flask (5 mL for 25 cm² flask, 14 mL for 75 cm² flask, 24 mL for 150 cm² flask) with growth medium. Then the flasks were incubated in humidified incubator 5% CO₂ at 37°C.

3.2.7.3. Freezing and Thawing Cultured Cells

All cell lines in continuous cultures are under contamination risk. Therefore it is important that the cells are stored by frozen down to prevent the contamination risk and enable to keep for long-term storage. In this study, for freezing the cells, firstly the cells were disrupted from cell culture flasks by trypsinization. The cell suspension was transferred into a sterile falcon tube and then centrifuged at 800 rpm for 5 minutes at room temperature. After centrifugation, the supernatant was carefully removed and the pellet was resuspended by the addition of freezing medium consists 7 mL of growth medium, 2 mL of Fetal Bovine Serum (FBS) and 1 mL Dimethyl Sulfoxide (DMSO). The cell suspension was transferred to the cryogenic vials (2 mL). Next, they were incubated at +4°C for 1 hour and then at -20°C for 1 hour and finally transferred to freezer -80°C for long-term storage.

For thawing the cells, the cryogenic vial was removed from freezer (-80°C) and carefully thawed in a water bath at 37°C to obtain more percentage of viable cells. When the cells melted (1-2 minutes), it was immediately transferred into a sterile filtered tissue culture flask (25cm²) and completed the volume of flask with 3-4 mL of growth medium and incubated at 37°C in 5% CO₂.

3.2.7.4. Cell Proliferation, Cytotoxicity and Cell Cycle Analysis

Due to the cell population's response to external factors, cell proliferation and viability profile can be determined by different in vitro assays. MTT assay is one of these in vitro assays bases on the measurement of the reduction of tetrazolium salts. Mitochondrial dehydrogenase enzyme in viable cells reduces the yellow tetrazolium salt and 3-[4,5-dimethylthiazol-2-yl]-3,5-diphenyl tetrazolium bromide dye (MTT) forms a purple formazan crystals (Figure 3.8) that can be quantified by spectrophotometric means (Stockert et al. 2012).

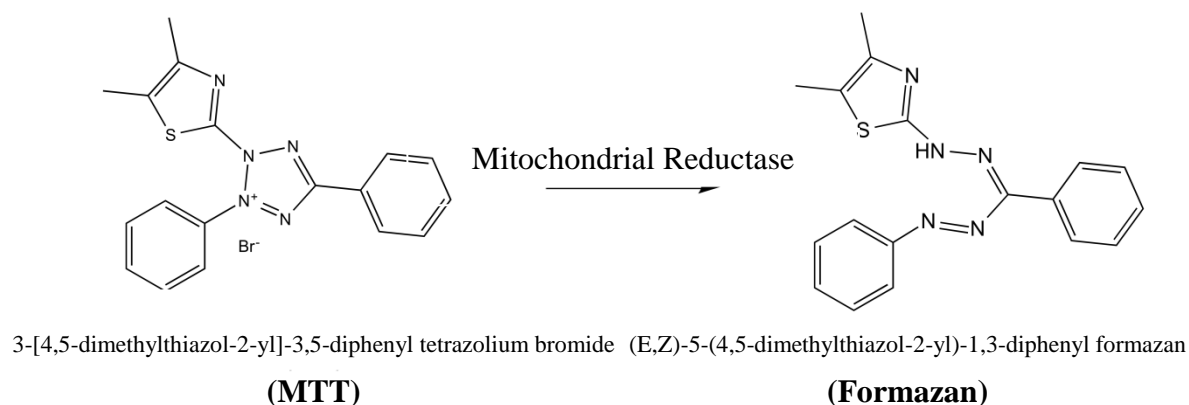


Figure 3.8. Mitochondrial reduction of MTT to purple Formazan.

In this study, MTT assay was performed to qualify the cell viability after incubated 24 h, 48 h and 72 h with different formulation 500:1, 300:1 and 100:1. Briefly; cells were seeded onto 96-well plates at a density of 3×10^3 (HeLa and MDA-MB-231) and 2×10^5 (THP-1) cells per well. At the end of each incubation time, the formulations were discarded and replaced with MTT-containing medium (500 $\mu\text{g/ml}$ working concentration). After second 4 h incubation at 37 °C, the medium was removed and formazan crystals were dissolved in DMSO (30 min, room temperature). Absorbance was read at 570 nm (measurement wavelength) and at 630 nm (reference wavelength) by Tecan Infinite® M200 absorbance mode microplate reader. Metabolic activity (activity of mitochondrial dehydrogenases) was calculated as a DA ($A_{570} - A_{630}$). Metabolic activity at standard growth conditions is considered as 100%.

The behavior of cells in a given cell cycle position quantitated by ImageJ 1.37v software (<http://rsb.info.nih.gov/ij/index.html>) with DAPI as staining markers, after 72 h treatment with CSNs-pDNA.

3.2.7.5. *In Vitro* Transfection Studies

Transfection is a process to introduce nucleic acids into cells by non-viral vectors. In this study, for the determination of the transfection efficiency cells were initially seeded onto 96-well plate at a density of 3×10^3 (HeLa and MDA-MB-231) and 2×10^5 (THP-1) cells per well and treated with CNs-pDNA at different weight ratios of 500:1, 300:1 and 100:1. After 24 h of incubation, the medium and complexes were

removed, media was replaced with 100 µl fresh medium containing serum and neomycin sulphate (1mg/ml) as selection agent.

The live cells were examined after 96 h with In Cell Analyzer 2000 (GE Healthcare, UK) equipped with a high performance CCD camera. Each transfection experiment was carried out as triplicate. Stable cell lines were obtained by continuous long-term culture in medium supplemented 1 mg/ml neomycin sulphate

$$\text{Transfection Efficiency (\%)} = \frac{\text{The number of transfected cells}}{\text{The total number of cells}} \times 100$$

3.2.7.6. Senescence-associated β-galactosidase activity (SA-β-gal)

Basically cellular senescence means to the essentially irreversible arrest of cell proliferation (growth) under potentially oncogenic stress (Campisi and d'Adda di Fagagna 2007). Senescence-associated β galactosidase activity can be detectable and senescent cells in culture or tissues can be determined at pH 6.0 (Debacq-Chainiaux et al. 2009). Herein, senescence-associated β galactosidase staining was performed as previously described (Mytych et al. 2014b).

For the detection of SA-β gal positive cells, cells were seeded onto 6-well plates at the density 10^4 (HeLa or MDA-MB-231) and 6×10^5 (THP-1) cells/well and after 72 h treatment with CNs-pDNA (500:1, 1%), they were fixed by fixation solution containing 2% formaldehyde, 0.2% glutaraldehyde for 5 min, room temperature. Then, cells were washed two times with PBS and staining solution was added (5 mM potassium ferrocyanide, 5 mM potassium ferricyanide, 150 mM NaCl, 2 mM MgCl₂, 1 mg/ml 5-bromo-4-chloro-3-indolyl-β-D-galactoside (X-gal), 40 mM citric acid/sodium phosphate, pH 6.0). After overnight incubation in 37°C, cells were washed with PBS and photographed with an Olympus BX71 light inverted microscope equipped with a DP72 CCD camera and a computer image analysis system Cell[^]b. SA-β-gal-positive cells were scored per 100 total cells analyzed [%].

3.2.7.7. Oxidative Stress

Oxidative stress associated with defected balance between the production of reactive oxygen species (free radicals) and antioxidant defences. The higher amount of ROS in the cells causes cellular damage in proteins, lipids and DNA. Therefore, ROS level plays a critical role in cellular physiopathology containing signalling pathways and cell proliferation (Forkink et al. 2010). In this study for the determination of total ROS production the 2', 7'-dichlorodihydrofluorescein diacetate (H₂DCF-DA) fluorescent probe that reacts with hydrogen peroxide, hydroxyl radicals and peroxynitrite was used.

For the determination of ROS level, cells were seeded at a density of 3×10^3 cells/cm² (HeLa and MDA-MB-231) and 2×10^5 cells/ml (THP-1) and treated for 72 h with (500:1, 1%) CNs-pDNA. Then, cells were washed and suspended in PBS containing 0.1% glucose, 0.5 mM EDTA and 5 μ M H₂DCF-DA as previously described (Mytych et al. 2014b). Fluorescence was monitored in a Tecan Infinite® M200 absorbance mode microplate reader at 495 nm (measurement wavelength) and at 525 nm (reference wavelength).

3.2.7.8. TUNEL Assay

One of the most characteristic key points of apoptosis is internucleosomal DNA fragmentation in mammalian cells. For the evaluation of DNA fragmentation (apoptotic-like change) in cells, Apo-BrdU TUNEL Assay Kit (BioVision) was performed with according to the manufacturer's instructions. This kit detects DNA fragmentation by Br-dUTP (bromolated deoxyuridine triphosphate nucleotides) which is more easily associated with DNA strand breaks than other larger ligands (e.g., fluorescein, biotin or digoxigenin). The bigger association cause rise to brighter signal when the Br-dUTP sites are detected by a fluorescein labeled antiBrdU monoclonal antibody. In this study, the cells were seeded at a density of 3×10^3 cells/cm² (HeLa and MDA-MB-231) and 2×10^5 cells/ml (THP-1). After 72 h treatment (500:1, 1%) CNs-pDNA, they were fixed by fixation solution containing 1% paraformaldehyde in PBS on ice for 15 min. Then, cells were washed two times with PBS and were resuspended in ice-cold 70% (v/v) ethanol for storage at -20°C freezer. On the day of analysis, aliquots were transferred to flow tubes and ethanol was removed by centrifugation (800XG for

15 min at RT). The cell suspension was washed with 1XWash Buffer (Apo-BrdU Kit) at 800x g for 15 min. The pellet was resuspended in freshly prepared DNA-labeling solution (Apo-BrdU Kit) as suggested by the manufacturer. The cell suspensions were incubated at 37°C in the dark for 2 hours. During the incubation, the cell suspensions were gently mixed at 30 min intervals. After incubation, the cell suspension was washed (800XG for 15 min at RT) in Rinse Buffer (Apo-BrdU Kit). The pellet transferred onto slides after it was resuspended in antibody solution as recommended by the manufacturer. After 30 minutes incubation, propidium iodide/RNase A solution was added to the cells and then incubated again in the dark for 30 min at room temperature. All slides were analyzed triplicate in an Olympus BX61 fluorescence microscope equipped with a DP72 CCD camera and Olympus CellF software.

3.2.7.10. Total Protein Extraction from the Cells

To extract total protein from the cells, HeLa, MDA-MB-231 and THP-1 cell lines were treated with the formulation of CNs-pDNA (500:1, 1% v/v) at a density of 1×10^5 cells/cm² for 72 h. For protein extraction, whole cell suspension was removed from tissue culture flask into a sterile falcon tube and then centrifuged at 500XG for 5 minutes at room temperature, separately. After centrifugation, the supernatant was discarded and the pellet washed with PBS and lyzed by RIPA buffer (50 mM Tris-HCl, pH 7.5, 1% NP-40, 0.5% sodium deoxycholate, 0.1% SDS, 150 mM NaCl, 1 mM PMSF, 1 mM EDTA and protease inhibitor) before incubated for 5 min on ice, then incubated on thermo-shaker (14.000 rpm, 4°C, 20 min). Next, the suspension was passed though a 21G needle 5 times and one more time incubated on thermo-shaker for 15 min. After that, the homogenates were centrifuged at 14000 rpm, 4°C for 15 min. Supernatant, which was the total protein of our samples, transferred to a fresh tube and stored at -80 °C before using for further studies.

3.2.7.11. Determination of Protein Concentration by BCA Assay

Protein concentrations of the samples were determined by using Pierce[®] BCA Protein Assay Kit with Bovine Serum Albumin (BSA) as standard. The principle of the assay associates with the measurement of the reduction of Cu²⁺ to Cu¹⁺ by protein in an

alkaline medium using bicinchoninic acid (BCA) which is the highly sensitive and selective colorimetric detection of the cuprous cation (Cu^{1+}) (Krohn 2001). For the determination of protein concentration 96 well-plates were used. After mixing of BCA working reagent BCA (A) and cooper II sulphate (B) at the ratio of 50:1 (A:B), 100 μL of the solution were added to each well. BSA stocks were prepared at different concentrations in RIPA buffer (10 mg/mL, 5 mg/mL, 1 mg/mL, 0,5 mg/mL, 0,25 mg/mL, 0,125 mg/mL and 0 mg/mL) to obtained BSA curve,. Next, 25 μL of protein samples and BSA stocks at different concentrations were added to the each well into the 100 μL BCA solutions. The plate incubated at at 5% CO_2 at 37°C for 30 min. Then absorbance was measured at 562 nm by a Tecan Infinite® M200. The protein concentration was calculated from standard curve, presented as ug/mL.

3.2.7.12. Western Blotting

Western blot is a technique that refers specifically to the immunological detection of proteins that have been separated by gel electrophoresis and transferred onto a membrane (Kurien and Scofield 2006). The basic principle of western blotting depends on separation proteins by electrophoresis on an SDS-polyacrylamide gel (SDS-PAGE). After that the samples are transferred to a PVDF (polyvinyl difluoride) or nitrocellulose membrane. The transferred protein can be detected and imaging by specific primary and enzyme labeled secondary antibody. In this study, for western blot analysis 5 steps were followed as sample preparation, gel electrophoresis, membrane transfer, immunoblotting and detection. Initially whole cell protein extracts were prepared according to Mytych et al. (Mytych et al. 2014a) for immunoblotting. The samples were added to laemmli buffer to denature proteins and then incubated at 95 °C for 5 minutes. After loaded samples on SDS PAGE gel consists stacking gel and separating gel in a single electrophoresis, allowed the separation of proteins for stacking gel at 80V for 15-30 min and for separating gel at 120V for 1- 1,5 h in 1X electrophoresis buffer . After total running time, proteins are transferred from the gel onto immobilon polyvinylidene difluoride (PVDF, Figure 3.9) where they become immobilized as a replica of the gel's band pattern (blotting) in 1X transfer buffer at 100 V for 100 minutes.

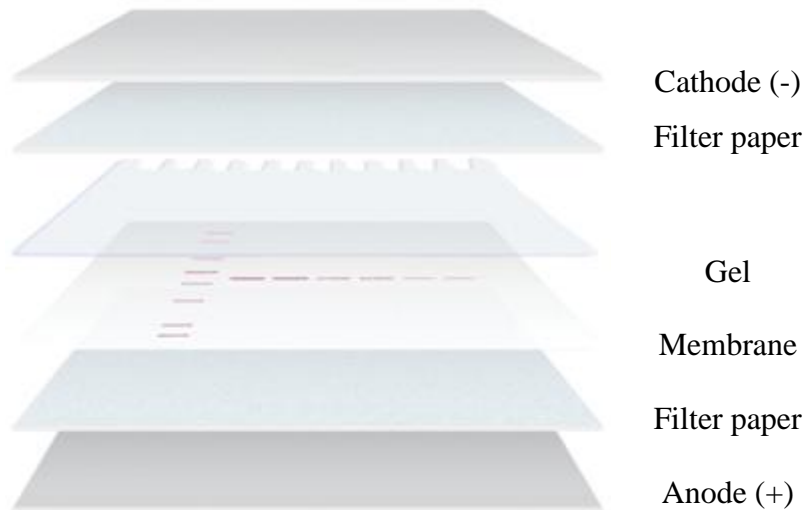


Figure 3.9. Gel and membrane preparation for electrophoretic transfer.
(Source: [Bio-Rad](#)).

After transferring, in order to block non-specific signals membranes were incubated in 3% BSA in TBST at room temperature for 1 hr. Proteins were detected using primary antibodies anti-p21 (1:100) (Abcam), anti-DNMT2 (1:500), and anti- β -actin (1:10000), (Thermo Scientific) for overnight in the primary antibody solution, against target protein, at 4° C. 4. The blots rinsed 3 times for 5 minutes with TBST before incubated with a secondary antibody conjugated to HRP (1:80000) in 1% BSA TBST for 1 hour. After incubation with secondary antibody, the blots rinsed again 3 times for 5 minutes with TBST. The protein bands visualization was conducted using the Pierce™ ECL Western Blotting Substrate (Life Technologies) and a G:BOX imaging system.

3.8. Statistical Analysis

Data were presented as mean \pm standart deviation from at least three independent experiments. All microscopic evaluations were performed on randomized and coded slides. Comparison between two groups was analyzed by one-way ANOVA with the Dunnett's multiple comparison test, and the difference was considered significant at $p < 0.05$.

CHAPTER 4

RESULTS AND DISCUSSION

4.1. Formation and Optimization of Chitosan Nanoparticles

The preparation of chitosan nanoparticles was based on an ionic gelation method that was reported previously by (Calvo et al. 1997). Ionic gelation method is more efficient than other formation methods for chitosan nanoparticles since the process is quite simple, mild and also avoids the use of harmful organic solvents and high temperatures. As a result it allows the encapsulation of critical molecules successfully (Al-Qadi et al. 2012; Berger et al. 2004; Nasti et al. 2009; Xu and Du 2003).

According to previously studies, the size of chitosan-plasmid DNA nanoparticle varies at the range of 50-500 nm (Mao et al. 2001; Masotti et al. 2008; Mao, Sun, and Kissel 2010). Determination of particle's size profile and zeta potential are significant since the biological performance of NPs influenced and thus they affect the mobility of vectors in the blood and uptake of vectors by cell membrane. To obtain efficient nanoparticles with optimal size and zeta potential for successful transfection, we synthesized initial chitosan nanoparticles (CNs). Dynamic light scattering (DLS) and laser doppler velocimetry (LDV) were used for the characterization of nanoparticles.

The use of chitosan nanoparticles for chitosan-plasmid DNA nanoparticles formation was available as preliminary study. In this way, several parameters such as different formulations (1:1, 2:1, 3:1, 4:1, 5:1, 6:1) of composed of chitosan (CS) and tripolyphosphate (TPP), also different pH (4.0, 4.5, 5.0, 5.5, 6.0) values were evaluated during the fabrication of the nanoparticle to vary the size and polydispersity index (P.I.). The particles which have optimal size, zeta potential and polydispersity index (P.I.) were selected for further experiments.

4.1.1. Effect of CS:TPP Mass Ratio

To evaluate the effects of CS:TPP mass ratio on particle size, different formulations at different ratio as 1:1, 2:1, 3:1, 4:1, 5:1 and 6:1 were analyzed at the pH of 5.0, 60 minutes incubation of TPP, at the temperature of 25°C. Results are presented in Figure 4.1 and Table 4.1.

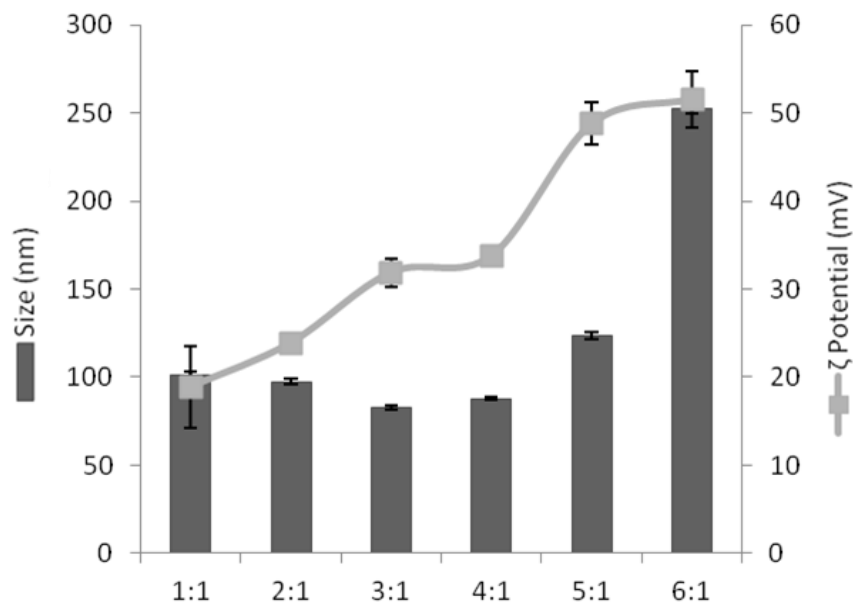


Figure 4.1. The effect of increasing CS:TPP mass ratios on the size of chitosan nanoparticles (n=3).

As observing in Figure 4.1, there is a tendency to increase the size of particles with the higher chitosan concentration, which have high amount of chitosan chain length inside. Similar result also reported by Gan et al. that the particle size is increased with the increasing CS:TPP mass ratio (Gan et al. 2005).

In addition, the particle aggregation become more rapidly and rigidly with higher amount of TPP. It was reported by Antonio and colleagues that TPP interacts with inter- and intra- molecular crosslinking. Therefore more TPP in the solution causes more aggregation and thus larger particles (Rampino et al. 2013). Similarly it was observed in the Figure 4.1 that the formulations (1:1 and 2:1) exhibit an increase in their size.

When the value of polydispersity index (P.I.) considered, Zhang and Kosaraju were reported that P.I. under 0.3 exhibits high homogeneity in the size of particles which in the dispersion (Zhang and Kosaraju 2007). Therefore in this study, the 4:1 ratio due to the P.I. of 0.333 was selected to further optimisation experiments (Table 4.1).

Table 4.1. Size, zeta potential and polydispersity index (P.I.) of the chitosan nanoparticles for different ratio of CS:TPP.

Formulation	Size (nm)	P.I.	ζ Potential (mV)
1:1	101.4±1.5	0.412	+18.9 ± 4.6
2:1	97.5±1.3	0.391	+23.9 ± 0.5
3:1	82.7±1.1	0.383	+31.9 ± 1.6
4:1	87.9±0.8	0.333	+33.8 ± 0.8
5:1	123.6±1.7	0.522	+48.8 ± 2.4
6:1	252.4±2.8	0.623	+51.6 ± 3.2

4.1.2. Effect of pH

Chitosan is considered as a strong base due to its amino groups with a pKa value of 6.2-7 (Ravi Kumar 1999). Chitosan is only soluble in acidic solution at a pH below 6 and its solubility increases as the pH decreases. Because at a low pH the amino groups of chitosan become protonated and thus the surface charge get positive allowing it to interact with negative materials (Pillai, Paul, and Sharma 2009; Roberts 1992).

Therefore, effect of pH on initial CS solution was investigated in our study. To determine the effect of initial pH value on CS solution on size of NPs, particles were formed at the CS:TPP mass ratio of 4:1, 60 minutes incubation TPP and at the temperature of 25°C. Results are presented in Figure 4.2 and Table 4.2.

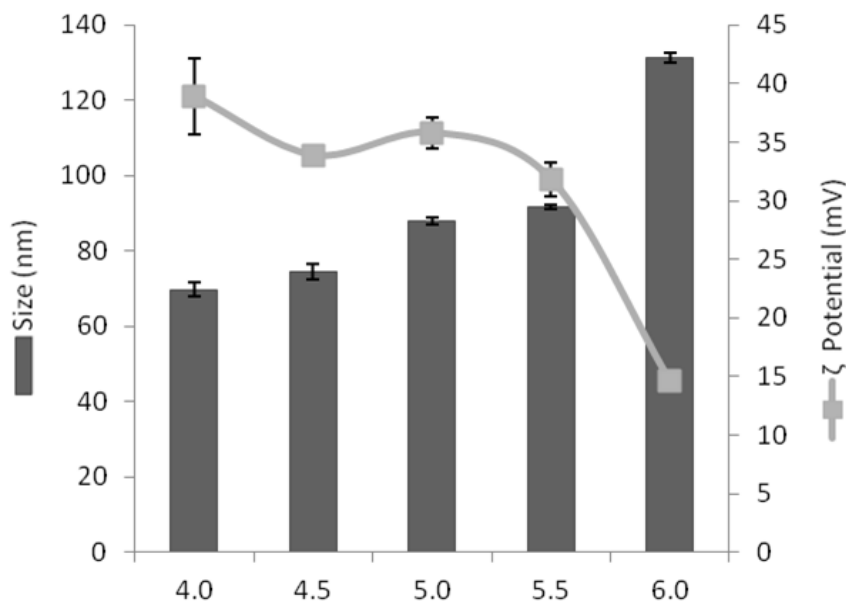


Figure 4.2. The effect of increasing pH values on the size of chitosan nanoparticles.

As can be observed in the Figure 4.2, the pH has an important role in the determination of size and zeta potential. Increasing the pH from 4.0 to the 6.0 resulted in sharp increases in size and reduction of particle stability.

According to Zhang et. al., the below pH 4.5 causes stronger protonation of the -NH₂ and thus stronger intra molecular repulsion with the TPP or other cross linking agent. On the other hand, higher pH than 4.5 causes weak protonation degree and thus larger nanoparticles (Zhang and Kosaraju 2007).

Table 4.2. Size, zeta potential and polydispersity index (P.I.) of the chitosan nanoparticles for different pH values.

pH	Size (nm)	P.I.	ζ Potential (mV)
4.0	69.8±1.9	0.380	+38.9 ± 3.2
4.5	74.5±2.1	0.393	+33.9 ± 0.8
5.0	87.9±0.8	0.333	+33.8 ± 0.8
5.5	91.7±0.6	0.214	+31.8 ± 1.4
6.0	131.4±1.3	0.362	+14.6 ± 0.2

The surface charge density of chitosan molecules is strongly dependent on solution pH. Zeta potential is significant parameter in biometaterials, medicine, pharmaceuticals, and water treatment (Lee, Powers, and Baney 2004). At the same time, the zeta potential measurements can be referred the stability and adhesion of the particles in biological systems. Particles have a zeta potential from -30 mV to +30 mV considered unstable (Zhang and Kosaraju 2007). Therefore in this study, the 4:1 ratio at the pH of 5.5 with the zeta potential of $+31.8 \pm 1.4$ and the P.I. of 0.214 was selected to synthesize chitosan-plasmid DNA nanoparticles for further experiments (Table 4.2).

4.2. Synthesis and Characterization of Chitosan-plasmid DNA Nanoparticles (CNs-pDNA)

The formation of CNs with pDNA was formulated using different CNs amount with fixed pDNA concentration and the formulated compounds were characterized by physically and chemically in details. The concentration of CS and pDNA in the mixed solution has a obvious effect on the particle size and zeta potential.

The size of CNs-pDNA nanoparticles was measured by dynamic light scattering (DLS). As shown in Table 4.3, the size of compounds were CNs amount-dependent as pDNA loading increased, size was increased as expected.

The zeta potential of CNs-pDNA nanoparticles was measured by laser Doppler velocimetry (LDV). Zeta potential indicated the value of the particle surface charge. In our study, a small reduction was observed in zeta potential according to increasing amount of the pDNA loading. As it was discussed previously, this could be explained by the presence of some negatively charged pDNA on to the surface of the nanoparticles (Csaba, Koping-Hoggard, and Alonso 2009). The methodology employed here resulted in high encapsulation efficiency of pDNA crosslinked chitosan nanoparticles independent of the CS:pDNA ratios. All formulated compounds were displayed more than 80% encapsulation efficiency.

Table 4.3. Physical and chemical characteristics of different CNs-pDNA formulation (500:1, 300:1 and 100:1). P.I.= polydispersity index.

Formulation	Size (nm)	P.I.	ζ Potential (mV)	Encapsulation efficiency (%)
500:1	220 \pm 7.2	0.581	+37.5 \pm 4.6	94.77 \pm 4.37
300:1	206 \pm 11.8	0.364	+33.8 \pm 1.8	97.42 \pm 2.03
100:1	164 \pm 13.4	0.341	+21.6 \pm 3.2	80.95 \pm 1.03

The shape of the CNs-pDNA was determined by atomic force microscope (AFM). All the formulated compounds with different pDNA loading have displayed similar well defined spherical particles and some unwanted aggregates (Figure 4.3). The heterogeneous morphology having suffered aggregates obtained in this study agrees with previously reported studies (Erbacher et al. 1998; Köping-Höggård et al. 2003).

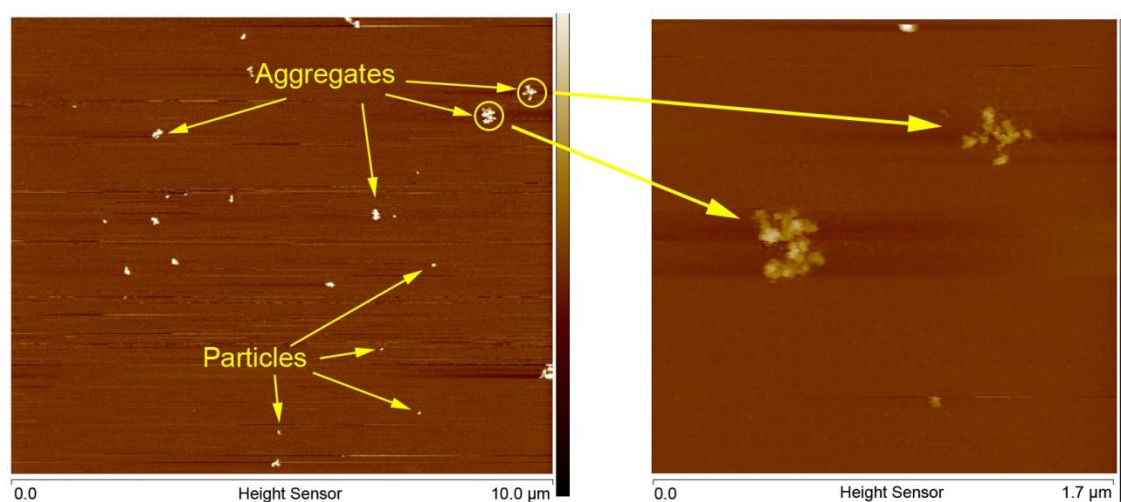


Figure 4.3. Typical topographic Height Sensor image of particles in suspension obtained by atomic force microscopy (AFM). Individual nanoparticles and their aggregates are indicated by arrows. Nanoparticles were kept in DMEM medium for up to 2 days prior to AFM analyses.

Gel electrophoresis studies were performed to assess the association/encapsulation of pDNA within nanoparticles (Figure 4.4). Binding efficiency between chitosan and pDNA at different CS:pDNA ratios were evaluated according to agarose gel retardation for 0 h, 24 h and 48 h.

As expected, all formulated compounds using different pDNA loading displayed a similar retardation results compared to single pDNA. The gel results also show that the binding efficiency was strong enough for at least 48 hours.

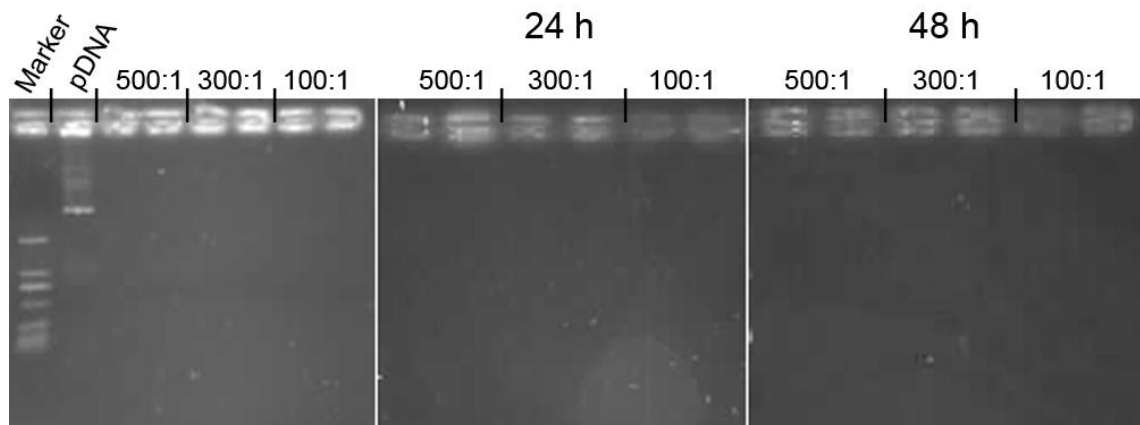


Figure 4.4. Binding efficiency between chitosan and pDNA at different CS:pDNA ratios by agarose gel retardation assay for 0 h, 24 h and 48 h.

4.3. Transfection Efficiency of CNS-pDNA

As a particulate carrier, CNS-pDNA containing multiple plasmids was well characterized and their transfection efficiency seems to be cell type-dependent (Corsi et al. 2003; Csaba, Koping-Hoggard, and Alonso 2009; Hallaj-Nezhadi et al. 2011; Mao et al. 2001). For example, Csaba et al. (2009) showed that CNS-pDNA complexes were uptaken through endocytosis by HEK293 cells and subsequent release into the cytoplasm occurred within 14h, while high gene expression levels were observed 2 days after transfection (Csaba, Koping-Hoggard, and Alonso 2009). Similarly, Hallaj-Nezhadi et al. (2011) presented 2.8 times improved transfection efficiency with the use of CNS-pDNA in comparison to naked pDNA (Hallaj-Nezhadi et al. 2011).

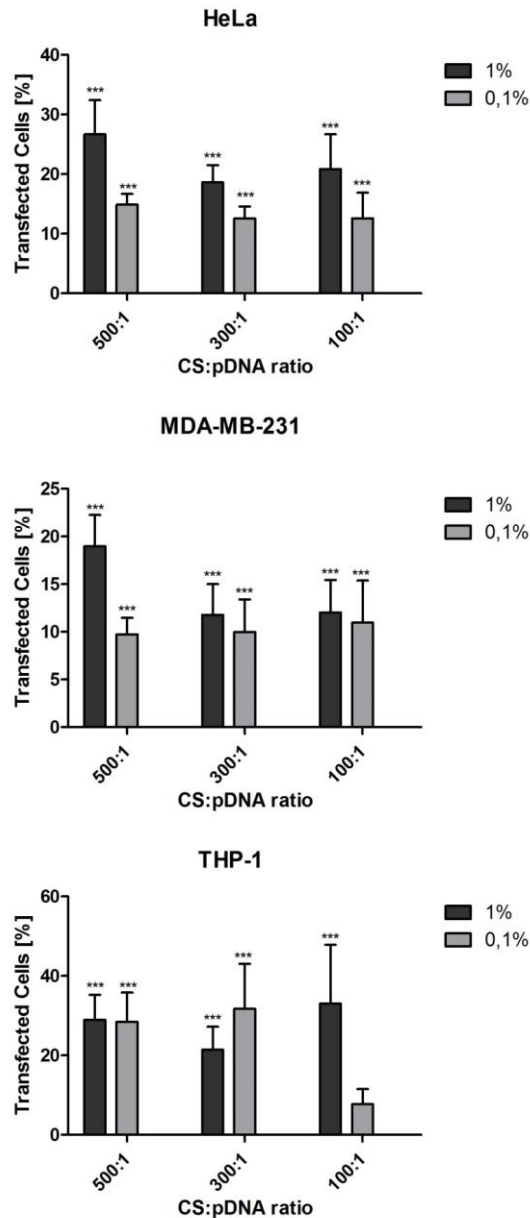


Figure 4.5. Transfection efficiency of CNs-pDNA formulations at different ratio of 500:1, 300:1 and 100:1 after 96 h of transfection. Bars indicate SD, n = 3, ***p<0.001.

In our study, we evaluated the efficiency of transfection with CNs-pDNA complexes (Figure 4.5). It was observed that the percentage of transfected cells after 96 h was 27%, 19% and 24% for HeLa, MDA-MB-231 and THP-1 respectively, while stable transfected cells were positive for fluorescent protein presence in almost 100% for all examined cell lines. As reported previously (Hallaj-Nezhadi et al. 2011), short-term transfection efficiency with CNs-pDNA was lower than using Lipofectamine 2000.

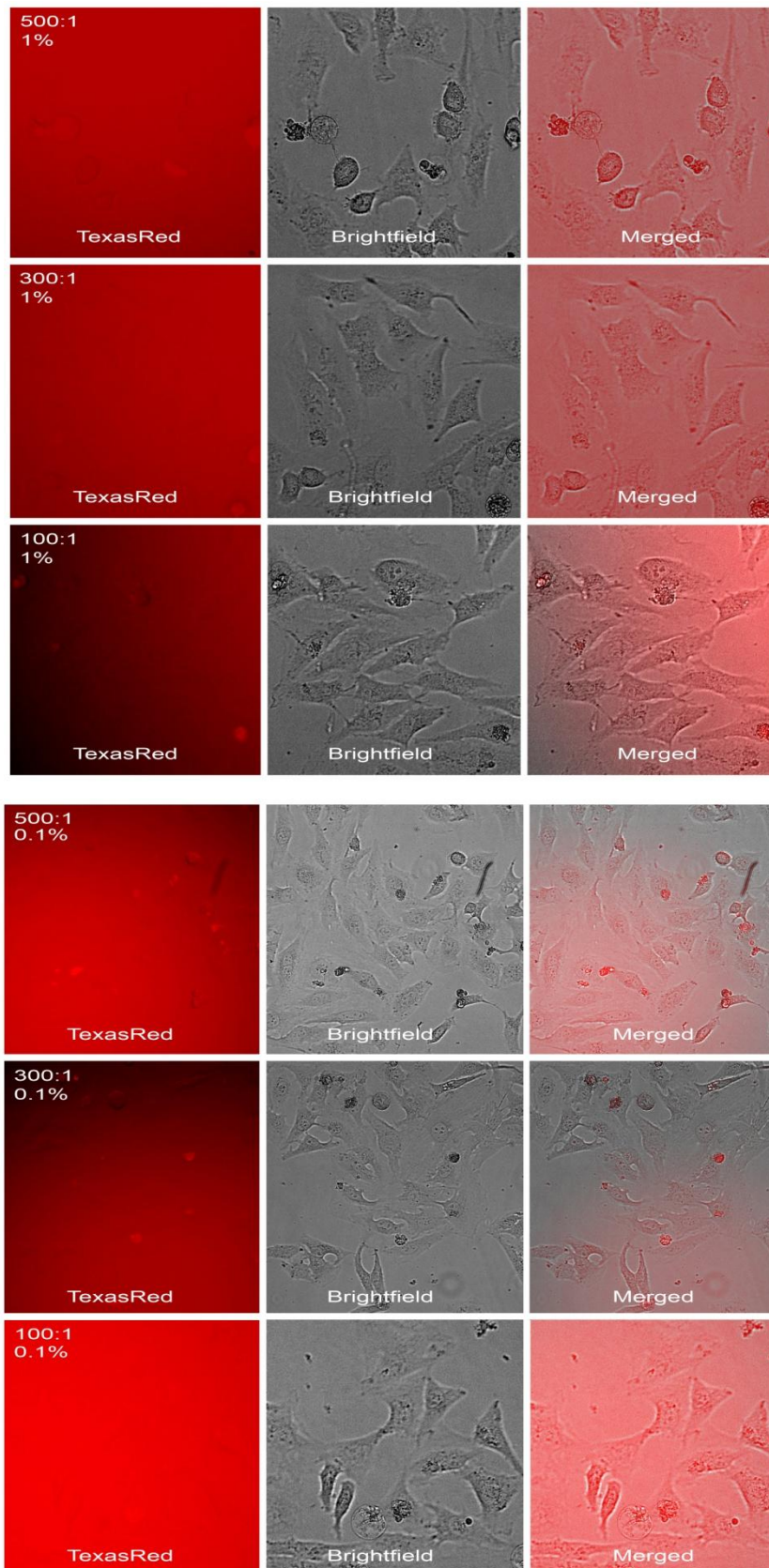


Figure 4.6. Typical kindling red fluorescent protein (KFP) expression in HeLa cell line with 1% and 0.1% CNs-pDNA, respectively.

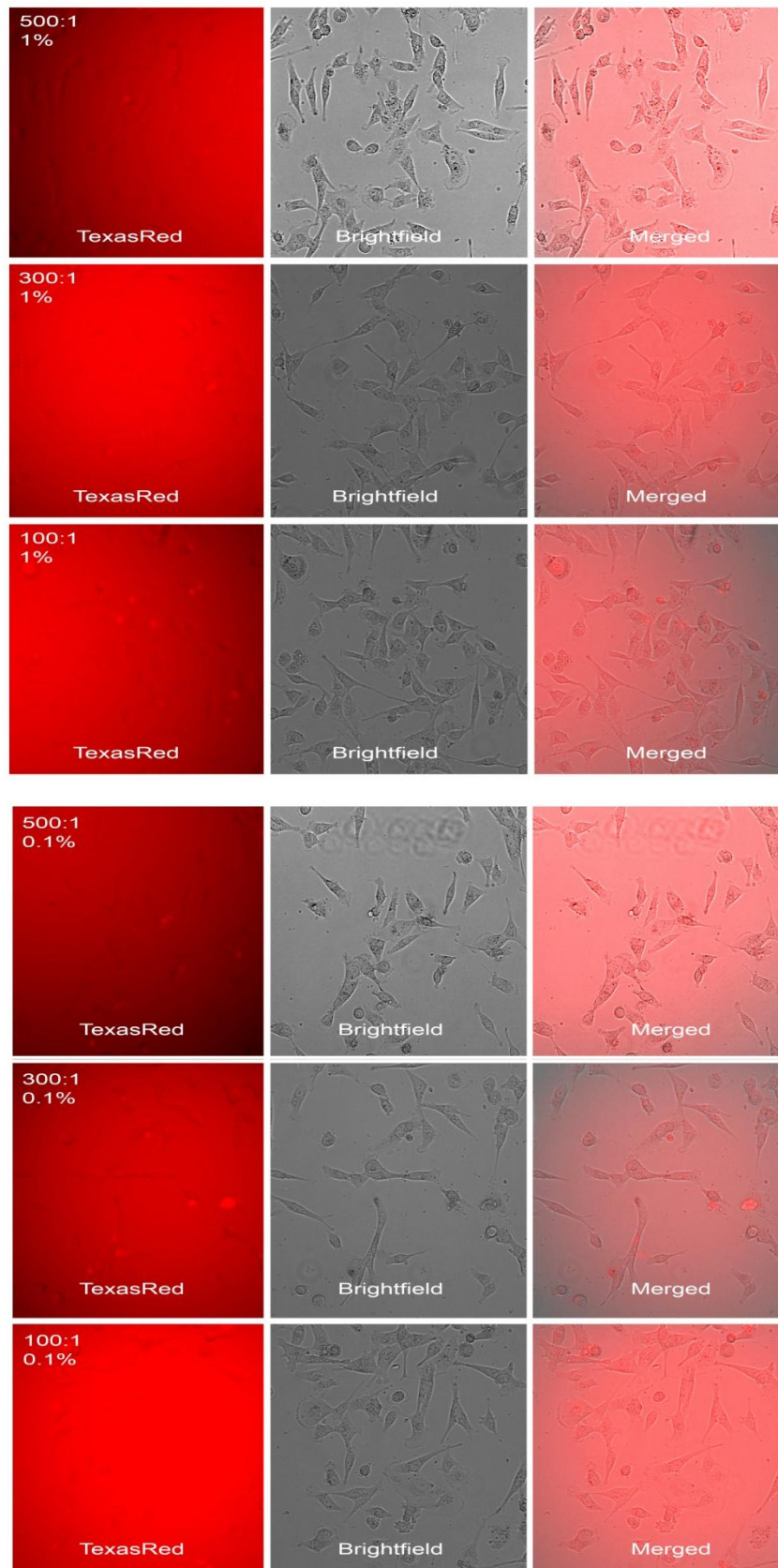


Figure 4.7. Typical kindling red fluorescent protein (KFP) expression in MDA-MB-231 cell line with 1% and 0.1% CNS-pDNA, respectively.

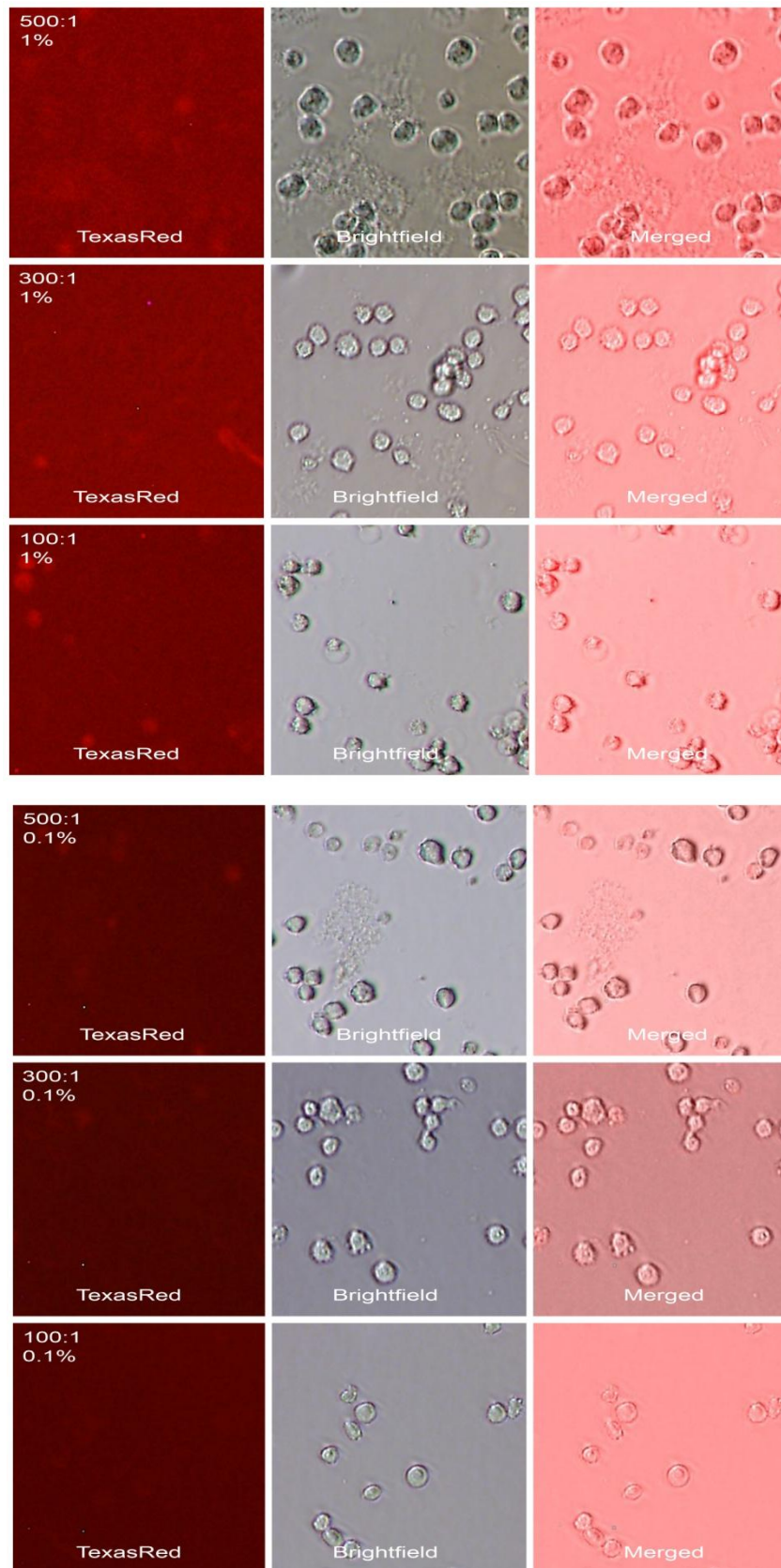


Figure 4.8. Typical kindling red fluorescent protein (KFP) expression THP-1 cell line with 1% and 0.1% CNs-pDNA, respectively.

4.4. Cell type-dependent Cytotoxic and Cytostatic Effect of CNs and CNs-pDNA

In the administration of CNs-pDNA particles, besides the transfection efficiency and gene expression, biocompatibility of the particles have to be considered as other biological factors. That was possible by the evaluation of the impact of synthesized CNs-pDNA used the concentrations of 10%, 5%, 1% and 0.1% on the metabolic activity of tested cells (Figure 4.9, 4.10 and 4.11). Thus in the first step of *in vitro* experiments we could decide to choose working concentration of CNs-pDNA for further studies. MTT assay was performed to qualify the cell viability after incubated 24 h, 48 h and 72 h with different formulation 500:1, 300:1 and 100:1. Results revealed that there are no differences between controls and treated for 24h, 48h and 72h cells in the case of HeLa and MDA-MB-231 cell lines. That is in agreement with previous studies done in different cell line models, i.e. mouse hematopoietic stem cells (Omar Zaki, Ibrahim, and Katas 2015), human respiratory epithelial cells (Grenha et al. 2007), human epithelial liver cells (Yang et al. 2014), mouse epithelial-like cells (Ragelle et al. 2014), mouse fibroblast colon cells (Hallaj-Nezhadi et al. 2011), human mesenchymal stem cells (Corsi et al. 2003) and human embryonic kidney cells (Corsi et al. 2003; Zhou et al. 2015). On the other hand, only a few reports showed inhibition in metabolic activity caused by CNs-pDNA treatment (Wimardhani et al. 2014; Yao et al. 2013).

Interestingly, in our study, THP-1 monocytic metabolic activity was reduced. Treatment with plain CNs decreased their metabolic activity to the same level irrespective of used concentration (to approximately 75 – 82%), while CNs-pDNA-triggered reduction was ratio- and concentration-dependent – observed variations may be due to methodological differences in CNs and CNs-pDNA preparation and different amounts of particular components (Figure 4.11).

Continuing, the most pronounced effect was observed for the lowest concentrations of 500:1 CNs-pDNA (inhibition to 60%) and the highest concentration of 300:1 and 100:1 CNs-pDNA (reduction to 54% and 51% respectively). The selection of working concentration for further studies was based on the interest in the identifying different responses underlying adaptation of various cells to the presence of CNs-pDNA in the environment.

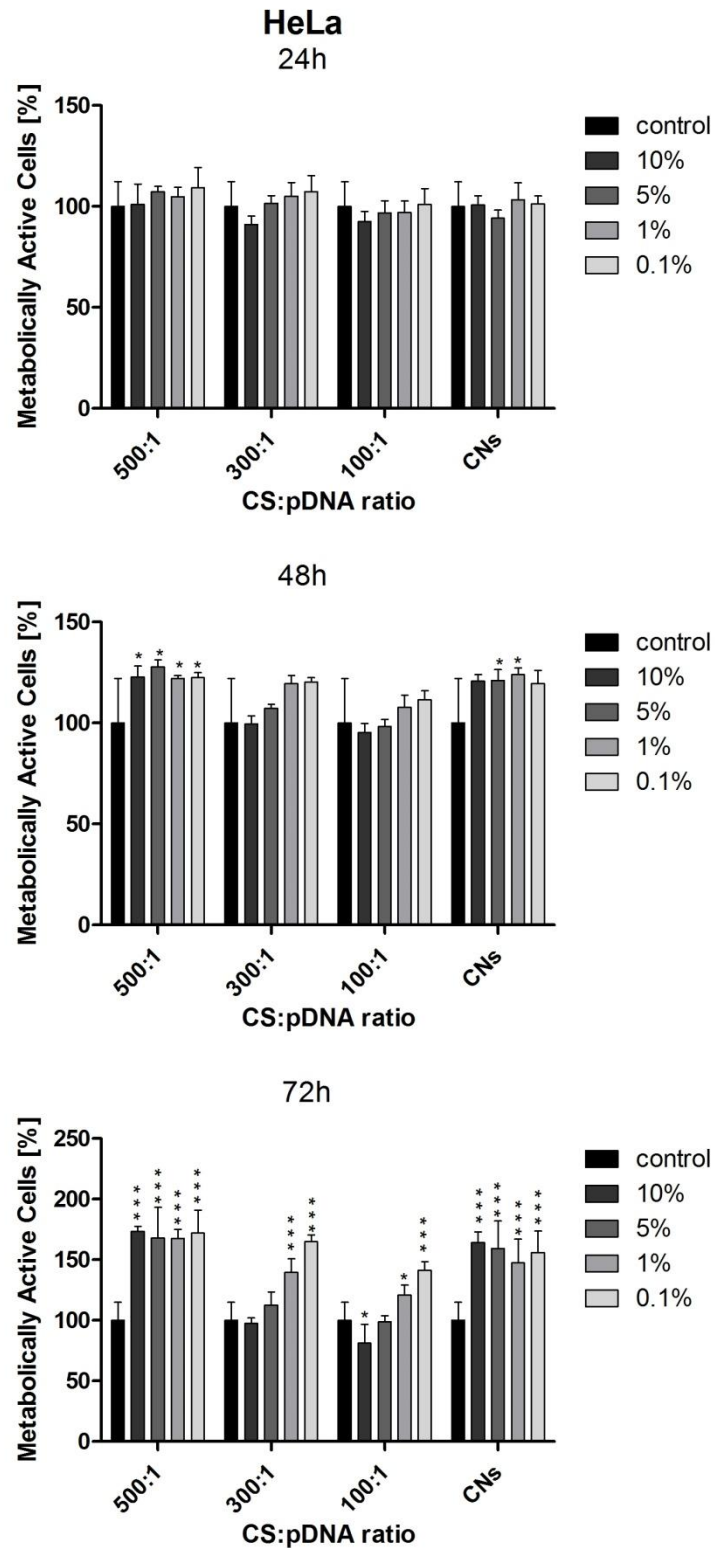


Figure 4.9. Metabolically active HeLa cells following exposure to CNs-pDNA for 24h, 48h and 72h treatment with different concentration with the ratio of 500:1, 300:1, 100:1 and ratios of CNs-pDNA. Bars indicate SD, n = 3, ***p<0.001, **p<0.01, *p<0.05.

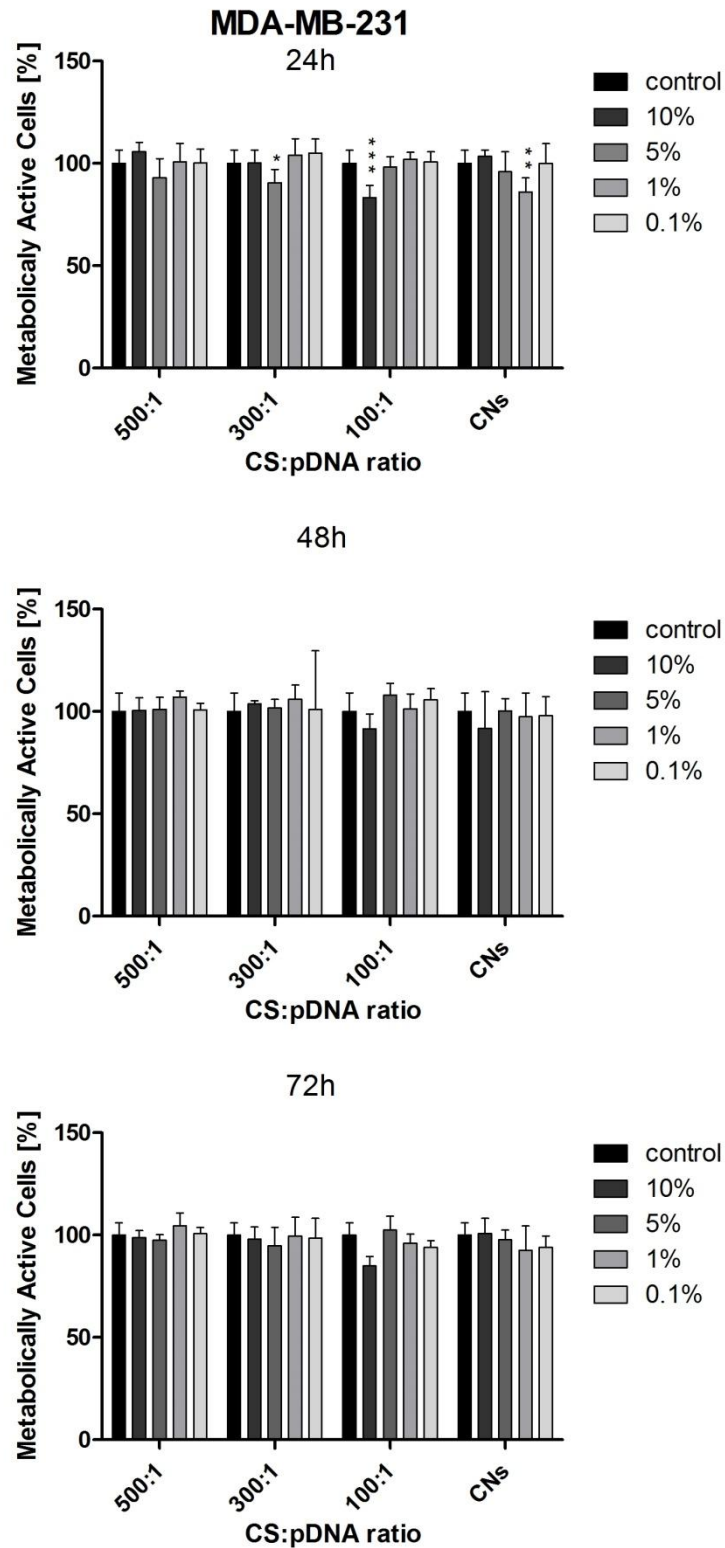


Figure 4.10. Metabolically active MDA-MB-231 cells following exposure to CNs-pDNA for 24h, 48h and 72h treatment with different concentration with the ratio of 500:1, 300:1, 100:1 and ratios of CNs-pDNA. Bars indicate SD, n = 3, ***p<0.001, **p<0.01, *p<0.05.

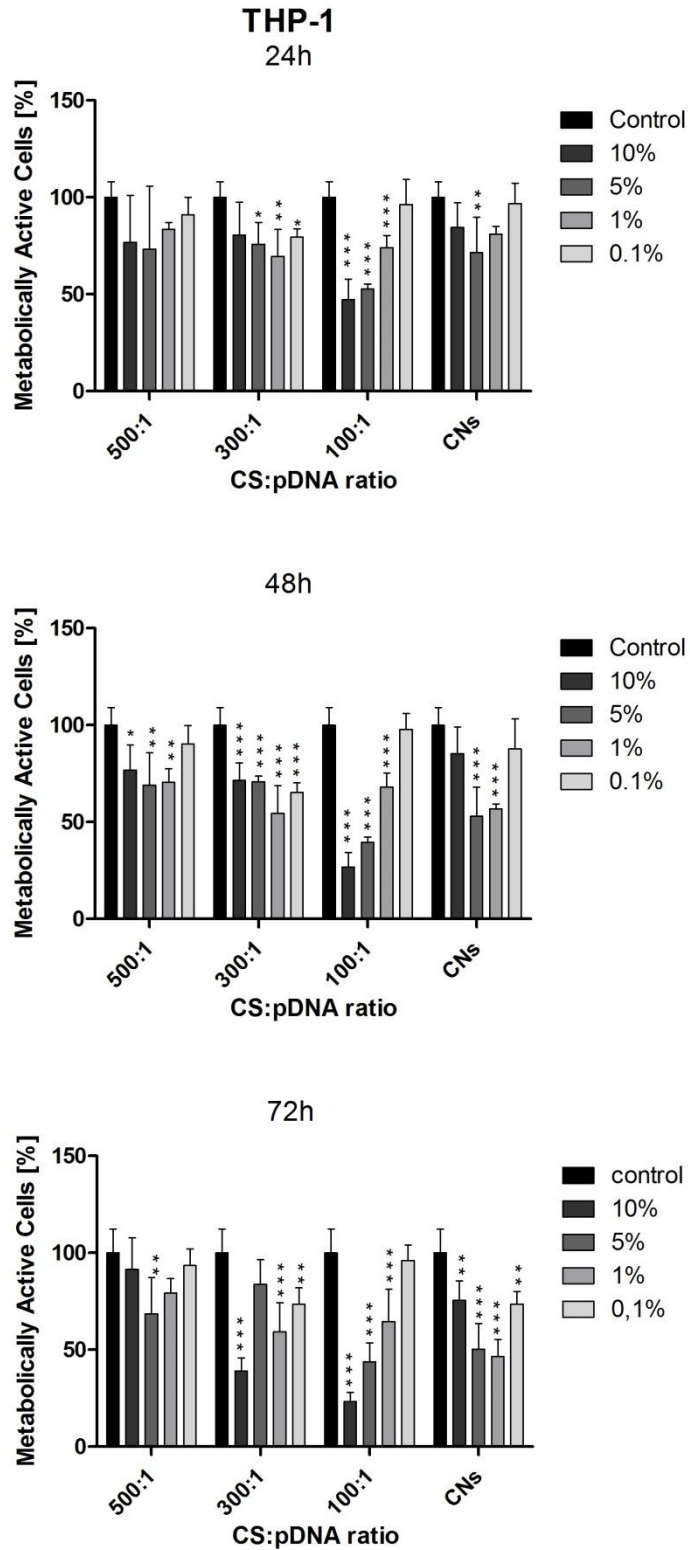


Figure 4.11. Metabolically active THP-1 cells following exposure to CNs-pDNA for 24h, 48h and 72h treatment with different concentration with the ratio of 500:1, 300:1, 100:1 and ratios of CNs-pDNA. Bars indicate SD, n = 3, ***p<0.001, **p<0.01, *p<0.05.

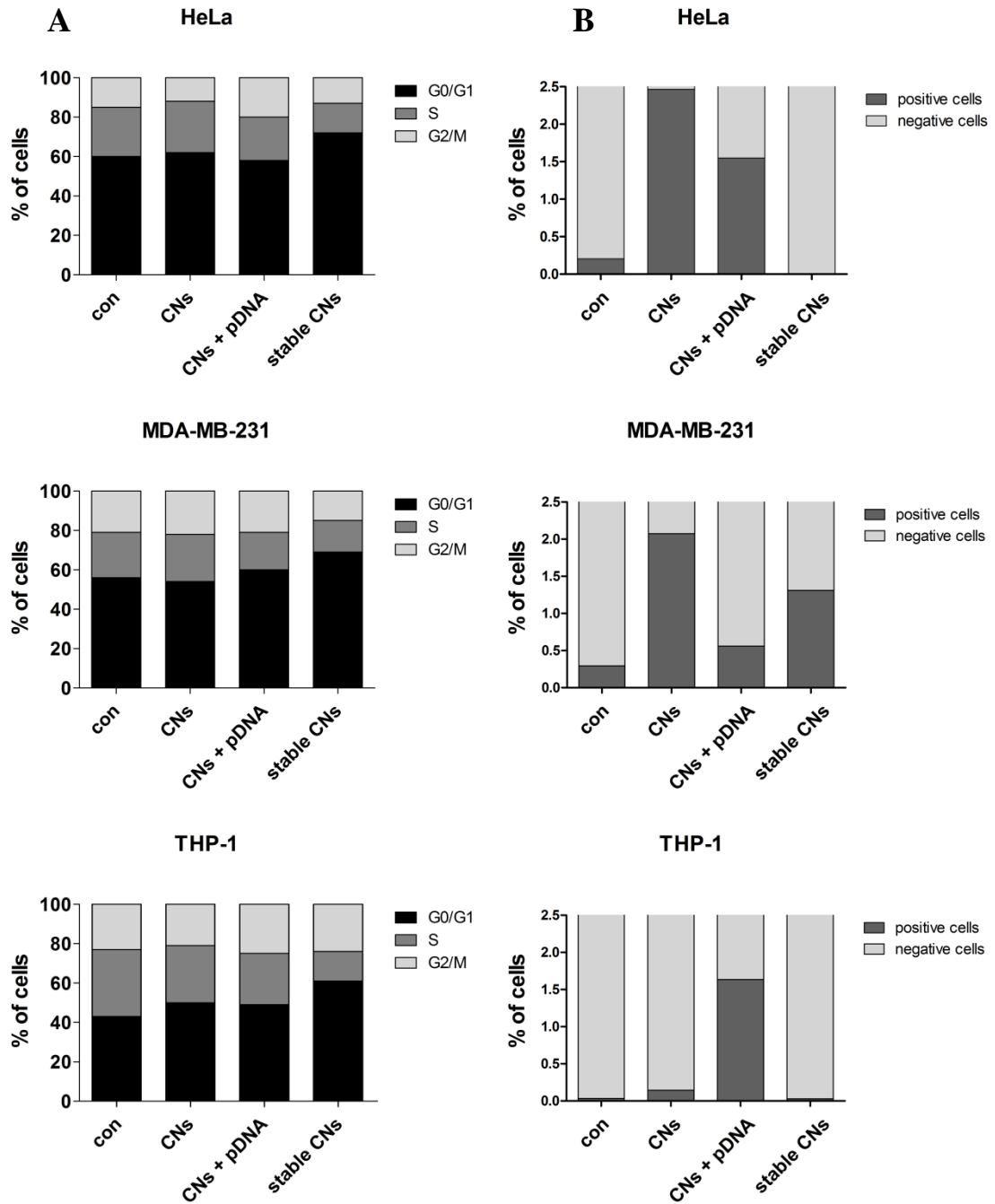


Figure 4.12. (A) Changes in the cell cycle profile due to the 72 h treatment with 1% (500:1) CNs-pDNA. (B) Changes in the DNA fragmentation profile due to the 72 h treatment with 1% (500:1) CNs-pDNA.

Then, we wanted to define mechanism leading to the reduction of the metabolic activity of THP-1 treated with CNs-pDNA, thus we decided to check whether that process is due to the proliferation inhibition or cell death (Figure 4.12A).

Therefore, we determined cell cycle profile and found these disruptions caused by 72 h treatment with CNs-pDNA. It was observed that the % of THP-1 cells in the G0/G1 phase increased and in the S phase decreased at the same time. Moreover, in all examined stable transfected cells we observed G0/G1 cell cycle arrest. At the same time, considerable apoptotic cell death did not take place (Figure 4.12B). That process seems to be also cell type-dependent. For instance, in HaCaT, but not Ca9-22 cells, caspase-independent apoptosis was induced. However, exposure to CNs resulted in a significant increase in the G1 phase population (from 33% to 51%) indicating cell cycle arrest in Ca9-22 cells (Wimardhani et al. 2014).

4.5. Oxidative stress-induced premature senescence

Since oxidative stress was linked with NPs-mediated toxicity (Manke, Wang, and Rojanasakul 2013; Mytych, Pacyk, et al. 2015) and affected cell cycle progression (Boonstra and Post 2004) we decided to check whether that process also takes place in applied conditions. Changes in generation of total ROS were monitored for evaluation of CNs-mediated oxidative stress induction in tested cells and their reduction was observed (Figure 4.13). Moreover, antioxidant activity of CNs was already coupled with their ability to suppress the production of lipid peroxidation, restore activity of endogenous antioxidant and increase total antioxidant capacity and was shown in *in vitro* (Wen et al. 2013) and *in vivo* (El-Denshary et al. 2015) models.

Continuing, it is widely accepted that irreversible cell cycle arrest may lead to stress-induced premature senescence (SIPS), characterised by cytomorphological and metabolic changes (Correia-Melo and Passos 2015). Moreover, recent findings suggest the possibility of induction of SIPS independently of ROS generation (Ziegler, Wiley, and Velarde 2015).

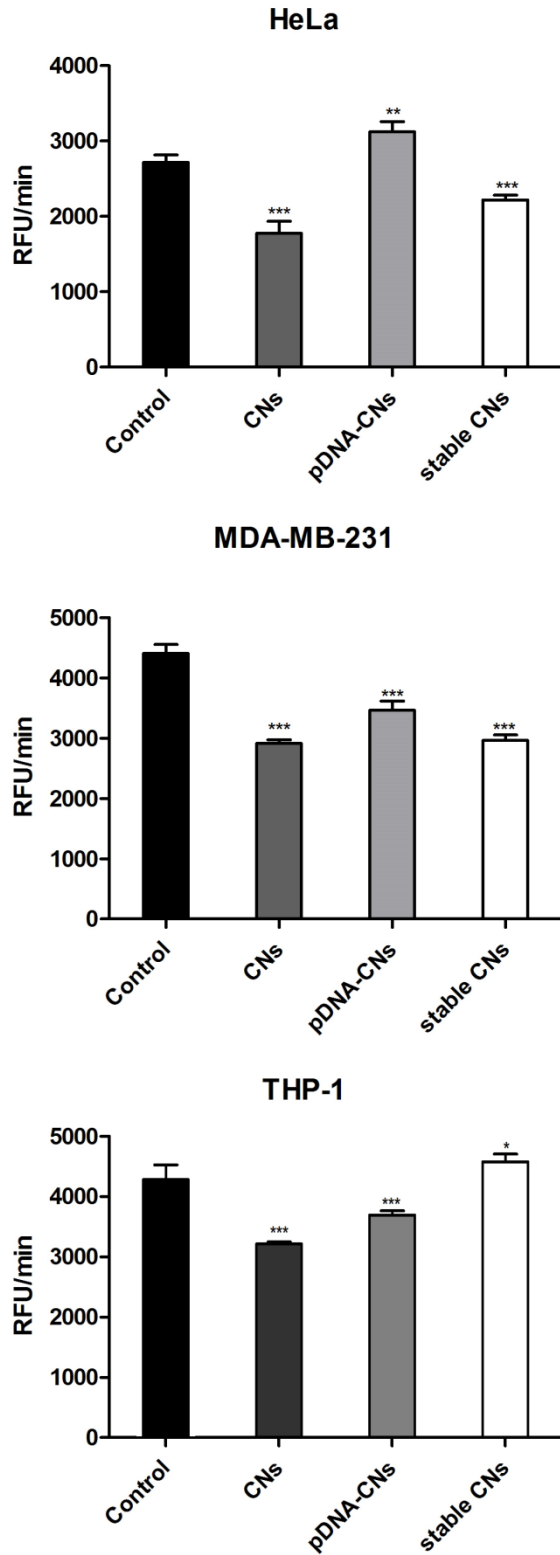


Figure 4.13. CNs-pDNA-mediated reduction in generation of total ROS. Bars indicate SD, n = 3, ***p<0.001, **p<0.01, *p<0.05.

In the present study, we noted the increase of the % of the cells positive for the presence of SA- β -gal, which widely serves as a senescence marker (Figure 4.14, Figure 4.15 and Figure 4.16). The most sensitive cell line was MDA-MB-231 with the 3 times increased population of SA- β -gal positive cells, while for HeLa and THP-1 the observed change was 1.6 and 2 times higher respectively.

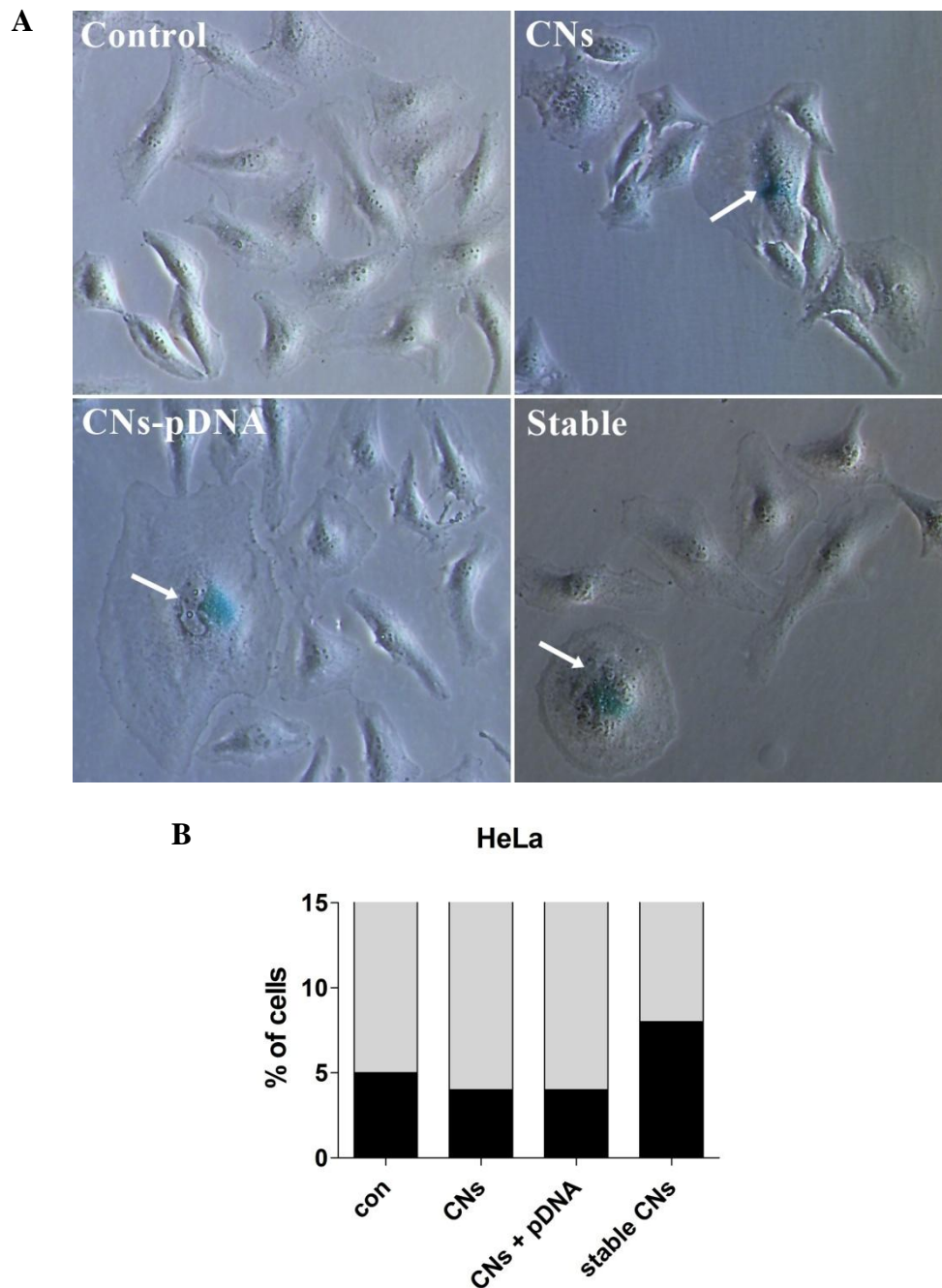
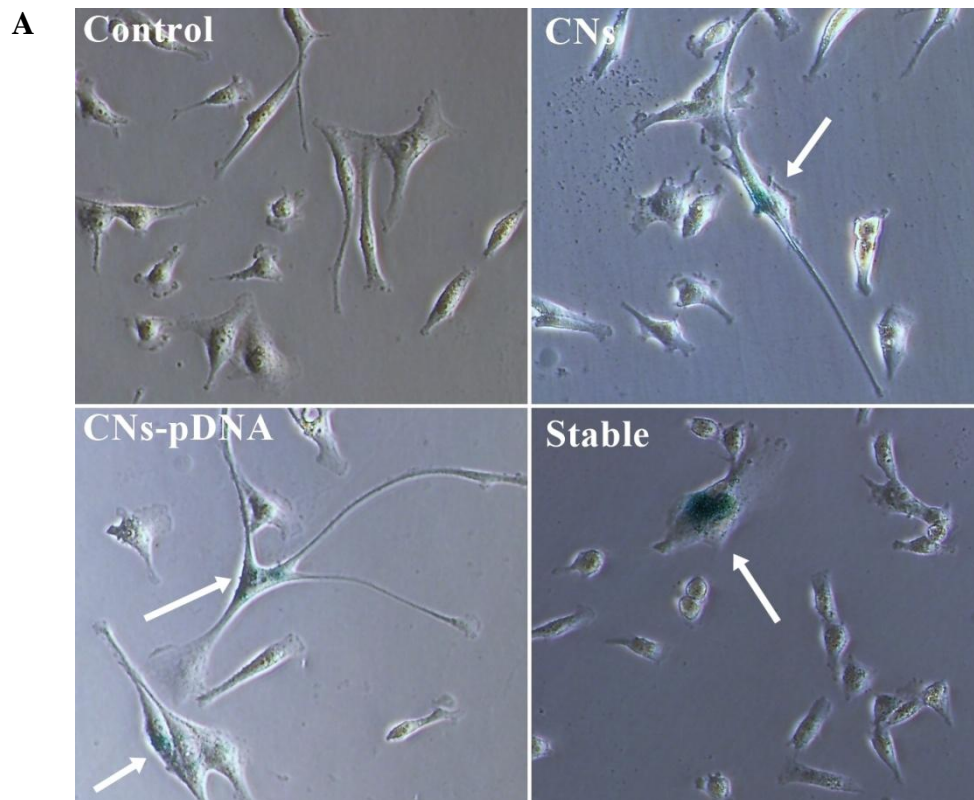


Figure 4.14. (A) Typical micrographs of SA- β -gal positive HeLa cells (B) CNs-pDNA-induced premature senescence in HeLa cells (microscopic magnification of the objective lens 10X).



B

MDA-MB-231

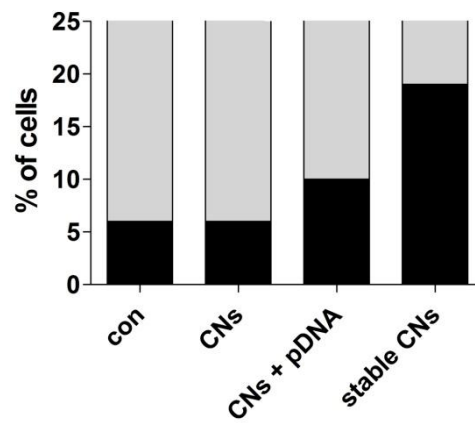


Figure 4.15. (A) Typical micrographs of SA- β -gal positive MDA-MB-231 cells (B) CNs-pDNA-induced premature senescence in MDA-MB-231 cells (microscopic magnification of the objective lens 10X).

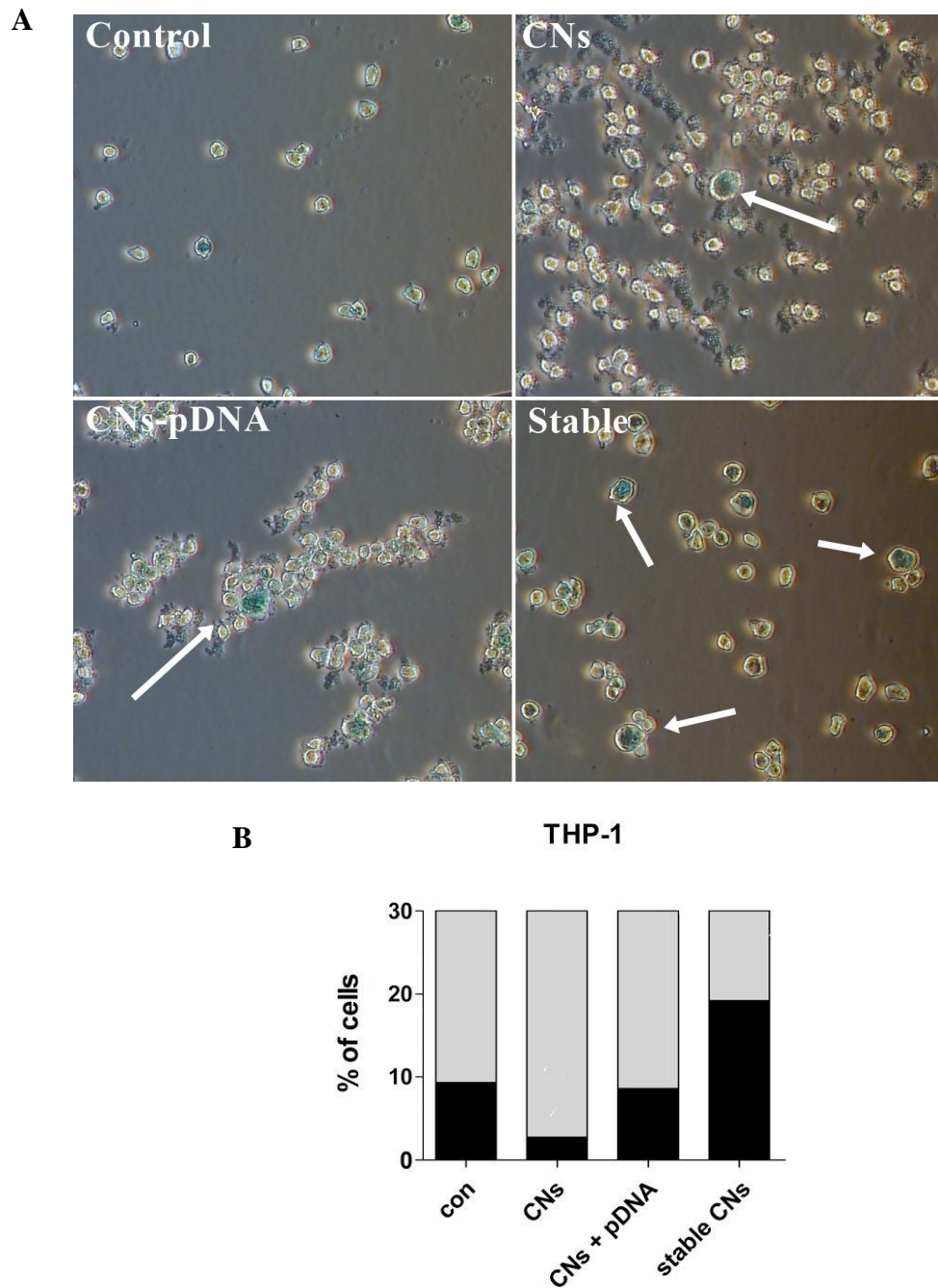


Figure 4.16. (A) Typical micrographs of SA- β -gal positive THP-1 cells (B) CNs-pDNA-induced premature senescence in THP-1 cells (microscopic magnification of the objective lens 10X).

Furthermore, the evaluation of the level of p21 protein, another widely known marker of senescence involved as well in cell cycle arrest, was also performed (Figure 4.15). It's up regulation was observed and the most pronounced effect was noted for MDA-MB-231 cell line.

Interestingly, it was already shown that NPs can induce both, p21-dependent and p21-independent, premature senescence (Mytych et al. 2014a; Mytych, Pacyk, et al. 2015) but here we report for the first time that observation in the context of CNs-pDNA. That process may be mediated by overexpression of TGF-beta 1 which further activates p15 and p21 and leads to cell cycle arrest, resulting in cellular senescence (Gong et al. 2003; Senturk et al. 2010). The possibility that SIPS was caused by overexpression of the gene carried by CNs-pDNA and protein accumulation was excluded due to the fact that expressed fluorescent protein was characterized as non-toxic and biologically inert (Henderson and Remington 2006). Furthermore, among many mechanisms engaged in senescence induction, also DNA and RNA methylation seems to play an important role (Machwe, Orren, and Bohr 2000; Oh, Jeong, and Cho 2015; So et al. 2011; Young and Smith 2001).

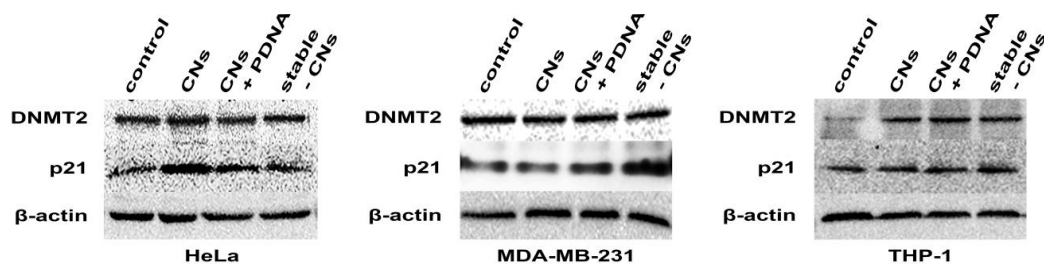


Figure 4.17. Effect of 1% 500:1 CNs-pDNA on protein expression profiles.

Besides that, DNA methyltransferase II (DNMT2), enzyme with the enigmatic role in the RNA methylation, was found to have protective role in the NPs-induced stress (Mytych et al. 2014a). Therefore, we decided to check whether CNs-pDNA treatment affects the pool of DNMT2 in tested cell lines and indeed, in THP-1 cells the level of DNMT2 was elevated (Figure 4.16). Perhaps, DNMT2 upregulation also in that case leads to RNA stabilization and confers stress resistance.

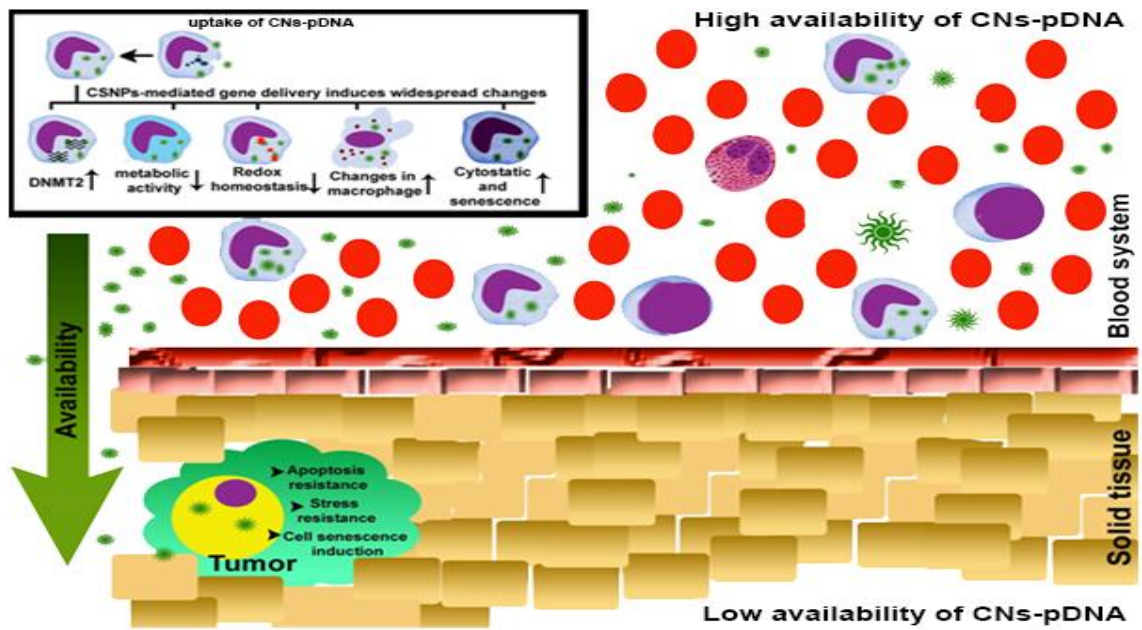


Figure 4.18. Due to the higher availability, cells belonging to the blood system are more susceptible to CNS-pDNA treatment than those derived from solid tissues.

CHAPTER 5

CONCLUSION

Chitosan-based gene delivery systems are widely studied in biomedical and pharmaceutical application. Despite the fact that, chitosan nanoparticles (CNs) are considered biocompatible, the studies about cytostatic or cytotoxic effects caused by biodegradable nanomaterials like CNs or/and type of used expression vector system on different cell types are still remain insufficient. In this context, due to the limited information on numerous cell lines interaction of chitosan based non-viral vectors, detailed investigations are required for comprehensive analysis of health risk assessment.

Through this project, we initially aimed to synthesize chitosan-plasmid DNA nanoparticles (CNs-pDNA) by ionic gelation method with the encapsulation of pKindlig-Red-Mito vector and then to evaluate their potential as safe-nanocarriers on different cell line models derived from human solid tissues cancers (HeLa and MDA-MB-231) and monocytes (derived from peripheral blood cancer – THP-1).

Nanoparticles based on chitosan for delivery of pKindling-red-Mito vector were successively generated by ionic gelation method at different ratio of CS:pDNA (500:1, 300:1, 100:1) with at least 80% encapsulation efficiency and high stability. The transfection efficiencies of particles were observed 27%, 19% and 24% for HeLa, MDA-MB-231 and THP-1 respectively by depended on formulation and cell-type. Moreover using different cell line models we showed that CNs-pDNA biocompatibility is limited and observed effects are cell-type dependent. Although THP-1 monocytic metabolic activity was reduced clearly, results showed that there are no significantly differences between controls and treated for 24h, 48h and 72h cells in the case of HeLa and MDA-MB-231 cell lines.

To understand which steps of cell cycle were affected by CNs-pDNA, cell cycle analyses were performed. Results showed that the % of THP-1 cells in the G0/G1 phase increased and in the S phase decreased at the same time, and also in all examined stable transfected cells we observed G0/G1 cell cycle arrest.

Moreover, another widely known marker of senescence, the level of p21 protein, involved as well in cell cycle arrest, was also evaluated. Results showed their up regulation especially in MDA-MB-231 cell line. At the same time, in our study, it was observed for the first time that CNs-pDNA can induce both, p21-dependent and p21-independent, premature senescence.

Besides p21 we checked also the CNs-pDNA treatment affects on DNMT2 in cell lines and indeed, in THP-1 cells the level of DNMT2 was elevated due to the RNA stabilization and confers stress resistance.

In summary, HeLa and MDA-MB-231 cell lines, which are derived from solid tumors and exhibit adherent properties in *in vitro* culture are probably more resistant to applied treatment than derived from blood THP-1 cells – perhaps due to limited availability of CNs-pDNA. Taking into account observed effects and the fact that monocytes are the first cells which are in contact with the CNs-pDNA after *in vivo* administration it is crucial to understand in detail these interactions before adopting proposed systems in biological and medical applications.

REFERENCES

- Agbulut, O., C. Coirault, N. Niederlander, A. Huet, P. Vicart, A. Hagege, M. Puceat, and P. Menasche. 2006. "GFP expression in muscle cells impairs actin-myosin interactions: implications for cell therapy." *Nat Methods* 3 (5):331.
- Agbulut, O., A. Huet, N. Niederlander, M. Puceat, P. Menasche, and C. Coirault. 2007. "Green fluorescent protein impairs actin-myosin interactions by binding to the actin-binding site of myosin." *J Biol Chem* 282 (14):10465-71.
- Agirre, Mireia, Jon Zarate, Edilberto Ojeda, Gustavo Puras, Jacques Desbrieres, and Jose Pedraz. 2014. "Low Molecular Weight Chitosan (LMWC)-based Polyplexes for pDNA Delivery: From Bench to Bedside." *Polymers* 6 (6):1727.
- Al-Qadi, S., A. Grenha, D. Carrion-Recio, B. Seijo, and C. Remunan-Lopez. 2012. "Microencapsulated chitosan nanoparticles for pulmonary protein delivery: in vivo evaluation of insulin-loaded formulations." *J Control Release* 157 (3):383-90. doi: 10.1016/j.jconrel.2011.08.008.
- Allin, Shawn B. 2004. "Polymer Science and Technology, 2nd Edition (Joel R. Fried)." *Journal of Chemical Education* 81 (6):809. doi: 10.1021/ed081p809.
- Anderson, W. F. 1992. "Human gene therapy." *Science* 256 (5058):808-13.
- Baens, M., H. Noels, V. Broeckx, S. Hagens, S. Fevery, A. D. Billiau, H. Vankelecom, and P. Marynen. 2006. "The dark side of EGFP: defective polyubiquitination." *PLoS One* 1:e54. doi: 10.1371/journal.pone.0000054.
- Bailon, P., A. Palleroni, C. A. Schaffer, C. L. Spence, W. J. Fung, J. E. Porter, G. K. Ehrlich, et al. 2001. "Rational design of a potent, long-lasting form of interferon: a 40 kDa branched polyethylene glycol-conjugated interferon alpha-2a for the treatment of hepatitis C." *Bioconjug Chem* 12 (2):195-202.
- Bailon, P., and C. Y. Won. 2009. "PEG-modified biopharmaceuticals." *Expert Opin Drug Deliv* 6 (1):1-16. doi: 10.1517/17425240802650568.
- Baltimore, D. 1988. "Gene therapy. Intracellular immunization." *Nature* 335 (6189):395-6. doi: 10.1038/335395a0.
- Berger, J., M. Reist, J. M. Mayer, O. Felt, N. A. Peppas, and R. Gurny. 2004. "Structure and interactions in covalently and ionically crosslinked chitosan hydrogels for biomedical applications." *Eur J Pharm Biopharm* 57 (1):19-34.
- Bio-Rad. "Western Blotting Membranes and Filter Paper". <<http://www.bio-rad.com/>>, (updated 2016).
- Boonstra, J., and J. A. Post. 2004. "Molecular events associated with reactive oxygen species and cell cycle progression in mammalian cells." *Gene* 337:1-13.
- Borchard, G. 2001. "Chitosans for gene delivery." *Adv Drug Deliv Rev* 52 (2):145-50.
- Borzelleca, Joseph F. 2000. "Paracelsus: Herald of Modern Toxicology." *Toxicological Sciences* 53 (1):2-4. doi: 10.1093/toxsci/53.1.2.
- Bottero, Jean-Yves, Mélanie Auffan, Daniel Borschnek, Perrine Chaurand, Jérôme Labille, Clément Levard, Armand Masion, Marie Tella, Jérôme Rose, and Mark

- R. Wiesner. 2015. "Nanotechnology, global development in the frame of environmental risk forecasting. A necessity of interdisciplinary researches." *Comptes Rendus Geoscience* 347 (1):35-42.
- Boussif, O., F. Lezoualc'h, M. A. Zanta, M. D. Mergny, D. Scherman, B. Demeneix, and J. P. Behr. 1995. "A versatile vector for gene and oligonucleotide transfer into cells in culture and in vivo: polyethylenimine." *Proc Natl Acad Sci U S A* 92 (16):7297-301.
- Calvo, P., C. Remuñán-López, J. L. Vila-Jato, and M. J. Alonso. 1997. "Novel hydrophilic chitosan-polyethylene oxide nanoparticles as protein carriers." *Journal of Applied Polymer Science* 63 (1):125-32.
- Campisi, Judith, and Fabrizio d'Adda di Fagagna. 2007. "Cellular senescence: when bad things happen to good cells." *Nat Rev Mol Cell Biol* 8 (9):729-40.
- Chellat, F., A. Grandjean-Laquerriere, R. Le Naour, J. Fernandes, L. Yahia, M. Guenounou, and D. Laurent-Maquin. 2005. "Metalloproteinase and cytokine production by THP-1 macrophages following exposure to chitosan-DNA nanoparticles." *Biomaterials* 26 (9):961-70.
- Correia-Melo, C., and J. F. Passos. 2015. "Mitochondria: Are they causal players in cellular senescence?" *Biochim Biophys Acta*.
- Corsi, K., F. Chellat, L. Yahia, and J. C. Fernandes. 2003. "Mesenchymal stem cells, MG63 and HEK293 transfection using chitosan-DNA nanoparticles." *Biomaterials* 24 (7):1255-64.
- Csaba, N., M. Koping-Hoggard, and M. J. Alonso. 2009. "Ionically crosslinked chitosan/tripolyphosphate nanoparticles for oligonucleotide and plasmid DNA delivery." *Int J Pharm* 382 (1-2):205-14.
- Dash, M., F. Chiellini, R. M. Ottenbrite, and E. Chiellini. 2011. "Chitosan—A versatile semi-synthetic polymer in biomedical applications." *Progress in Polymer Science* 36 (8):981-1014.
- Debacq-Chainiaux, Florence, Jorge D. Erusalimsky, Judith Campisi, and Olivier Toussaint. 2009. "Protocols to detect senescence-associated beta-galactosidase (SA-[beta]gal) activity, a biomarker of senescent cells in culture and in vivo." *Nat. Protocols* 4 (12):1798-806.
- Dewey, R. A., G. Morrissey, C. M. Cowsill, D. Stone, F. Bolognani, N. J. F. Dodd, T. D. Southgate, et al. 1999. "Chronic brain inflammation and persistent herpes simplex virus 1 thymidine kinase expression in survivors of syngeneic glioma treated by adenovirus-mediated gene therapy: Implications for clinical trials." *Nat Med* 5 (11):1256-63.
- Donaldson, K, V Stone, C L Tran, W Kreyling, and P J A Borm. 2004. "Nanotoxicology." *Occupational and Environmental Medicine* 61 (9):727-8.
- Dumitriu, S. 2001. *Polymeric Biomaterials, Revised and Expanded*: CRC Press.
- . 2004. *Polysaccharides: Structural Diversity and Functional Versatility, Second Edition*: CRC Press.
- El-Denshary, E.S., A. Aljawish, A.A. El-Nekeety, N.S. Hassan, R.H. Saleh, B.H. Rihn, and M.A. Abdel-Wahhab. 2015. "Possible synergistic effect and antioxidant

- properties of chitosan nanoparticles and quercetin against carbon tetrachloride induce hepatotoxicity in rats." *Soft Nanoscience Letters* 5:36-51.
- Elsaesser, Andreas, and C. Vyvyan Howard. 2012. "Toxicology of nanoparticles." *Advanced Drug Delivery Reviews* 64 (2):129-37.
- Erbacher, Patrick, Shaomin Zou, Thierry Bettinger, Anne-Marie Steffan, and Jean-Serge Remy. 1998. "Chitosan-Based Vector/DNA Complexes for Gene Delivery: Biophysical Characteristics and Transfection Ability." *Pharmaceutical Research* 15 (9):1332-9.
- European Medicines Agency. 2010. "Gene Therapy". <<http://www.ema.europa.eu/>>, (accessed May 20th).
- Evrogen. 2002. "pKindling-Red-Mito Vector". <<http://www.evrogen.com/products/vectors/pKFP-Red-mito/pKFP-Red-mito.shtml>>, (accessed 2016).
- Ferraro, Bernadette, Matthew P. Morrow, Natalie A. Hutnick, Thomas H. Shin, Colleen E. Lucke, and David B. Weiner. 2011. "Clinical Applications of DNA Vaccines: Current Progress." *Clinical Infectious Diseases* 53 (3):296-302.
- Forkink, Marleen, Jan A. M. Smeitink, Roland Brock, Peter H. G. M. Willems, and Werner J. H. Koopman. 2010. "Detection and manipulation of mitochondrial reactive oxygen species in mammalian cells." *Biochimica et Biophysica Acta (BBA) - Bioenergetics* 1797 (6-7):1034-44.
- Fu, P. P., Q. Xia, H. M. Hwang, P. C. Ray, and H. Yu. 2014. "Mechanisms of nanotoxicity: generation of reactive oxygen species." *J Food Drug Anal* 22 (1):64-75.
- Gan, Q., T. Wang, C. Cochrane, and P. McCarron. 2005. "Modulation of surface charge, particle size and morphological properties of chitosan-TPP nanoparticles intended for gene delivery." *Colloids Surf B Biointerfaces* 44 (2-3):65-73. doi: 10.1016/j.colsurfb.2005.06.001.
- Gong, J., S. Ammanamanchi, T. C. Ko, and M. G. Brattain. 2003. "Transforming growth factor beta 1 increases the stability of p21/WAF1/CIP1 protein and inhibits CDK2 kinase activity in human colon carcinoma FET cells." *Cancer Res* 63 (12):3340-6.
- Grenha, A., C. I. Grainger, L. A. Dailey, B. Seijo, G. P. Martin, C. Remunan-Lopez, and B. Forbes. 2007. "Chitosan nanoparticles are compatible with respiratory epithelial cells in vitro." *Eur J Pharm Sci* 31 (2):73-84.
- Hallaj-Nezhadi, S., H. Valizadeh, S. Dastmalchi, B. Baradaran, M.B. Jalali, F. Dobakhtti, and F. Loftipour. 2011. "Preparation of chitosan-plasmid DNA nanoparticles encoding interleukin-12 and their expression in CT-26 colon carcinoma cells." *J Pharm PharmaceutSci* 14 (2):181-95.
- Henderson, J. N., and S. J. Remington. 2006. "The kindling fluorescent protein: a transient photoswitchable marker." *Physiology (Bethesda)* 21:162-70.
- Hillaireau, H., and P. Couvreur. 2009. "Nanocarriers' entry into the cell: relevance to drug delivery." *Cell Mol Life Sci* 66 (17):2873-96.

- Huang, M., C. W. Fong, E. Khor, and L. Y. Lim. 2005. "Transfection efficiency of chitosan vectors: effect of polymer molecular weight and degree of deacetylation." *J Control Release* 106 (3):391-406.
- Huang, W. Y., J. Aramburu, P. S. Douglas, and S. Izumo. 2000. "Transgenic expression of green fluorescence protein can cause dilated cardiomyopathy." *Nat Med* 6 (5):482-3. doi: 10.1038/74914.
- Ibraheem, D., A. Elaissari, and H. Fessi. 2014. "Gene therapy and DNA delivery systems." *International Journal of Pharmaceutics* 459 (1–2):70-83.
- Illum, L. 1998. "Chitosan and its use as a pharmaceutical excipient." *Pharm Res* 15 (9):1326-31.
- Ishii, T., Y. Okahata, and T. Sato. 2001a. "Mechanism of cell transfection with plasmid/chitosan complexes." *Biochim Biophys Acta* 1514 (1):51-64.
- Ishii, Tsuyoshi, Yoshio Okahata, and Toshinori Sato. 2001b. "Mechanism of cell transfection with plasmid/chitosan complexes." *Biochimica et Biophysica Acta (BBA) - Biomembranes* 1514 (1):51-64.
- Iwashita, S., Y. Hiramatsu, T. Otani, C. Amano, M. Hirai, K. Oie, E. Yuba, K. Kono, M. Miyamoto, and K. Igarashi. 2012. "Polyamidoamine dendron-bearing lipid assemblies: their morphologies and gene transfection ability." *J Biomater Appl* 27 (4):445-56.
- Jang, Mi-Kyeong, Byeong-Gi Kong, Young-Il Jeong, Chang Hyung Lee, and Jae-Woon Nah. 2004. "Physicochemical characterization of α -chitin, β -chitin, and γ -chitin separated from natural resources." *Journal of Polymer Science Part A: Polymer Chemistry* 42 (14):3423-32.
- Jin, Lian, Xin Zeng, Ming Liu, Yan Deng, and Nongyue He. 2014. "Current Progress in Gene Delivery Technology Based on Chemical Methods and Nano-carriers." *Theranostics* 4 (3):240-55.
- Johnston, S. A., A. M. Talaat, and M. J. McGuire. 2002. "Genetic immunization: what's in a name?" *Arch Med Res* 33 (4):325-9.
- Kamat, Prashant V., and Dan Meisel. 2003. "Nanoscience opportunities in environmental remediation." *Comptes Rendus Chimie* 6 (8–10):999-1007.
- Katas, Haliza, and H. Oya Alpar. 2006. "Development and characterisation of chitosan nanoparticles for siRNA delivery." *Journal of Controlled Release* 115 (2):216-25.
- Kean, T., and M. Thanou. 2010. "Biodegradation, biodistribution and toxicity of chitosan." *Adv Drug Deliv Rev* 62 (1):3-11.
- Khalil, I. A., K. Kogure, H. Akita, and H. Harashima. 2006. "Uptake pathways and subsequent intracellular trafficking in nonviral gene delivery." *Pharmacol Rev* 58 (1):32-45. doi: 10.1124/pr.58.1.8.
- Kiang, T., J. Wen, H. W. Lim, and K. W. Leong. 2004. "The effect of the degree of chitosan deacetylation on the efficiency of gene transfection." *Biomaterials* 25 (22):5293-301. doi: 10.1016/j.biomaterials.2003.12.036.
- Koike, M., Y. Yutoku, and A. Koike. 2013. "Ku80 attenuates cytotoxicity induced by green fluorescent protein transduction independently of non-homologous end joining." *FEBS Open Bio* 3:46-50.

- Köping-Höggård, M., Y. S. Mel'nikova, K. M. Vårum, B. Lindman, and P. Artursson. 2003. "Relationship between the physical shape and the efficiency of oligomeric chitosan as a gene delivery system in vitro and in vivo." *The Journal of Gene Medicine* 5 (2):130-41. doi: 10.1002/jgm.327.
- Kumirska, Jolanta, Mirko X. Weinhold, Jorg Thöming, and Piotr Stepnowski. 2011. "Biomedical Activity of Chitin/Chitosan Based Materials—Influence of Physicochemical Properties Apart from Molecular Weight and Degree of N-Acetylation." *Polymers* 3 (4):1875.
- Kurien, B. T., and R. H. Scofield. 2006. "Western blotting." *Methods* 38 (4):283-93. doi: 10.1016/j.ymeth.2005.11.007.
- Kurita, K. 2006. "Chitin and chitosan: functional biopolymers from marine crustaceans." *Mar Biotechnol (NY)* 8 (3):203-26.
- Kurita, Keisuke, Shigeru Ishii, Koji Tomita, Shin-Ichiro Nishimura, and Kayo Shimoda. 1994. "Reactivity characteristics of squid β -chitin as compared with those of shrimp chitin: High potentials of squid chitin as a starting material for facile chemical modifications." *Journal of Polymer Science Part A: Polymer Chemistry* 32 (6):1027-32.
- Lavertu, M., S. Methot, N. Tran-Khanh, and M. D. Buschmann. 2006. "High efficiency gene transfer using chitosan/DNA nanoparticles with specific combinations of molecular weight and degree of deacetylation." *Biomaterials* 27 (27):4815-24. doi: 10.1016/j.biomaterials.2006.04.029.
- Lee, Chul-Joo, Dietram A. Scheufele, and Bruce V. Lewenstein. 2005. "Public Attitudes toward Emerging Technologies: Examining the Interactive Effects of Cognitions and Affect on Public Attitudes toward Nanotechnology." *Science Communication* 27 (2):240-67.
- Lee, Dong-Won, Kevin Powers, and Ronald Baney. 2004. "Physicochemical properties and blood compatibility of acylated chitosan nanoparticles." *Carbohydr Polym* 58 (4):371-7.
- Lim, Mi Jung, Sang-Hyun Min, Jae-Jung Lee, Il Chul Kim, Ji Tae Kim, Dong Chul Lee, Nam-Soon Kim, et al. 2006. "Targeted Therapy of DNA Tumor Virus-Associated Cancers Using Virus-Activated Transcription Factors." *Mol Ther* 13 (5):899-909.
- Liu, H. S., M. S. Jan, C. K. Chou, P. H. Chen, and N. J. Ke. 1999. "Is green fluorescent protein toxic to the living cells?" *Biochem Biophys Res Commun* 260 (3):712-7.
- Liu, X., K. A. Howard, M. Dong, M. O. Andersen, U. L. Rahbek, M. G. Johnsen, O. C. Hansen, F. Besenbacher, and J. Kjems. 2007. "The influence of polymeric properties on chitosan/siRNA nanoparticle formulation and gene silencing." *Biomaterials* 28 (6):1280-8. doi: 10.1016/j.biomaterials.2006.11.004.
- Lu, Z. R. 2010. "Molecular imaging of HPMA copolymers: visualizing drug delivery in cell, mouse and man." *Adv Drug Deliv Rev* 62 (2):246-57. doi: 10.1016/j.addr.2009.12.007.
- Lv, Pengju, Yuezhen Bin, Yongqiang Li, Ru Chen, Xuan Wang, and Baoyan Zhao. 2009. "Studies on graft copolymerization of chitosan with acrylonitrile by the redox system." *Polymer* 50 (24):5675-80.

- MacGregor, Rob Roy, Jean D. Boyer, Kenneth E. Ugen, Kim E. Lacy, Stephen J. Gluckman, Mark L. Bagarazzi, Michael A. Chattergoon, et al. 1998. "First Human Trial of a DNA-Based Vaccine for Treatment of Human Immunodeficiency Virus Type 1 Infection: Safety and Host Response." *Journal of Infectious Diseases* 178 (1):92-100. doi: 10.1086/515613.
- Machwe, A., D. K. Orren, and V. A. Bohr. 2000. "Accelerated methylation of ribosomal RNA genes during the cellular senescence of Werner syndrome fibroblasts." *FASEB J* 14 (12):1715-24.
- MacLaughlin, Fiona C., Russell J. Mumper, Jijun Wang, Jenna M. Tagliaferri, Inder Gill, Mike Hinchcliffe, and Alain P. Rolland. 1998. "Chitosan and depolymerized chitosan oligomers as condensing carriers for in vivo plasmid delivery." *Journal of Controlled Release* 56 (1–3):259-72.
- Manke, A., L. Wang, and Y. Rojanasakul. 2013. "Mechanisms of nanoparticle-induced oxidative stress and toxicity." *Biomed Res Int* 2013:942916. doi: 10.1155/2013/942916.
- Malvern Instruments. 2011. "Dynamic Light Scattering (DLS)". <<http://www.malvern.com>>, (updated 2016).
- Mannell, Hanna, Joachim Pircher, Franziska Fochler, Yvonn Stampnik, Thomas Räthel, Bernhard Gleich, Christian Plank, et al. "Site directed vascular gene delivery in vivo by ultrasonic destruction of magnetic nanoparticle coated microbubbles." *Nanomedicine: Nanotechnology, Biology and Medicine* 8 (8):1309-18.
- Mao, H. Q., K. Roy, V. L. Troung-Le, K. A. Janes, K. Y. Lin, Y. Wang, J. T. August, and K. W. Leong. 2001. "Chitosan-DNA nanoparticles as gene carriers: synthesis, characterization and transfection efficiency." *J Control Release* 70 (3):399-421.
- Mao, Shirui, Wei Sun, and Thomas Kissel. 2010. "Chitosan-based formulations for delivery of DNA and siRNA." *Advanced Drug Delivery Reviews* 62 (1):12-27.
- Masotti, A., F. Bordi, G. Ortaggi, F. Marino, and C. Palocci. 2008. "A novel method to obtain chitosan/DNA nanospheres and a study of their release properties." *Nanotechnology* 19 (5):055302.
- Matsumoto, Y., K. Itaka, T. Yamasoba, and K. Kataoka. 2009. "Intranuclear fluorescence resonance energy transfer analysis of plasmid DNA decondensation from nonviral gene carriers." *J Gene Med* 11 (7):615-23.
- McCrudden, C. M., and McCarthy, H. O. 2013. "Cancer gene therapy—key biological concepts in the design of multifunctional non-viral delivery systems." *Gene Therapy-Tools and Potential Applications*, 81-84.
- Miyata, Kanjiro, Nobuhiro Nishiyama, and Kazunori Kataoka. 2012. "Rational design of smart supramolecular assemblies for gene delivery: chemical challenges in the creation of artificial viruses." *Chemical Society Reviews* 41 (7):2562-74.
- Mizutani, T., N. Kato, M. Hirota, K. Sugiyama, A. Murakami, and K. Shimotohno. 1995. "Inhibition of hepatitis C virus replication by antisense oligonucleotide in culture cells." *Biochem Biophys Res Commun* 212 (3):906-11.
- Mosser, David M., and Justin P. Edwards. 2008. "Exploring the full spectrum of macrophage activation." *Nat Rev Immunol* 8 (12):958-69.

- Mytych, J., A. Lewinska, A. Bielak-Zmijewska, W. Grabowska, J. Zebrowski, and M. Wnuk. 2014a. "Nanodiamond-mediated impairment of nucleolar activity is accompanied by oxidative stress and DNMT2 upregulation in human cervical carcinoma cells." *Chem Biol Interact* 220:51-63.
- Mytych, J., A. Lewinska, J. Zebrowski, and M. Wnuk. 2015. "Nanodiamond-induced increase in ROS and RNS levels activates NF- κ B and augments thiol pools in human hepatocytes." *Diamond and Related Materilas* 55:95-101.
- Mytych, J., K. Pacyk, M. Pepek, J. Zebrowski, A. Lewinska, and M. Wnuk. 2015. "Nanoparticle-mediated decrease of lamin B1 pools promotes a TRF protein-based adaptive response in cultured cells." *Biomaterials* 53:107-16.
- Mytych, Jennifer, Anna Lewinska, Anna Bielak-Zmijewska, Wioleta Grabowska, Jacek Zebrowski, and Maciej Wnuk. 2014b. "Nanodiamond-mediated impairment of nucleolar activity is accompanied by oxidative stress and DNMT2 upregulation in human cervical carcinoma cells." *Chemico-Biological Interactions* 220:51-63.
- Nasti, A., N. M. Zaki, P. de Leonardis, S. Ungphaiboon, P. Sansongsak, M. G. Rimoli, and N. Tirelli. 2009. "Chitosan/TPP and chitosan/TPP-hyaluronic acid nanoparticles: systematic optimisation of the preparative process and preliminary biological evaluation." *Pharm Res* 26 (8):1918-30.
- Nishina, K., T. Unno, Y. Uno, T. Kubodera, T. Kanouchi, H. Mizusawa, and T. Yokota. 2008. "Efficient in vivo delivery of siRNA to the liver by conjugation of alpha-tocopherol." *Mol Ther* 16 (4):734-40.
- Oberdörster, Eva. 2004. "Manufactured Nanomaterials (Fullerenes, C(60)) Induce Oxidative Stress in the Brain of Juvenile Largemouth Bass." *Environmental Health Perspectives* 112 (10):1058-62.
- Oh, Y. S., S. G. Jeong, and G. W. Cho. 2015. "Anti-senescence effects of DNA methyltransferase inhibitor RG108 in human bone marrow mesenchymal stromal cells." *Biotechnol Appl Biochem*.
- Omar Zaki, S. S., M. I. Ibrahim, and H. Katas. 2015. "Particle size affects concentration-dependent cytotoxicity of chitosan nanoparticles towards mouse hematopoietic stem cells." *Journal of Nanotechnology* 2015.
- Parker, Alan L., Christopher Newman, Simon Briggs, Leonard Seymour, and Paul J. Sheridan. 2003. "Nonviral gene delivery: techniques and implications for molecular medicine." *Expert Reviews in Molecular Medicine* 5 (22):1-15.
- Perez-Martinez, F. C., J. Guerra, I. Posadas, and V. Cena. 2011. "Barriers to non-viral vector-mediated gene delivery in the nervous system." *Pharm Res* 28 (8):1843-58. doi: 10.1007/s11095-010-0364-7.
- Pillai, C. K. S., Willi Paul, and Chandra P. Sharma. 2009. "Chitin and chitosan polymers: Chemistry, solubility and fiber formation." *Progress in Polymer Science* 34 (7):641-78.
- Ragelle, H., R. Riva, G. Vandermeulen, B. Naeye, V. Pourcelle, C. S. Le Duff, C. D'Haese, et al. 2014. "Chitosan nanoparticles for siRNA delivery: Optimizing formulation to increase stability and efficiency." *Journal of Controlled Release* 176:54-63.

- Rampino, Antonio, Massimiliano Borgogna, Paolo Blasi, Barbara Bellich, and Attilio Cesàro. 2013. "Chitosan nanoparticles: Preparation, size evolution and stability." *International Journal of Pharmaceutics* 455 (1–2):219-28.
- Ravi Kumar, M. N. V. 1999. "Chitin and chitosan fibres: A review." *Bulletin of Materials Science* 22 (5):905-15. doi: 10.1007/BF02745552.
- Ravi Kumar, Majeti N. V. 2000. "A review of chitin and chitosan applications." *Reactive and Functional Polymers* 46 (1):1-27.
- Ravina, M., E. Cubillo, D. Olmeda, R. Novoa-Carballal, E. Fernandez-Megia, R. Riguera, A. Sanchez, A. Cano, and M. J. Alonso. 2010. "Hyaluronic acid/chitosan-g-poly(ethylene glycol) nanoparticles for gene therapy: an application for pDNA and siRNA delivery." *Pharm Res* 27 (12):2544-55.
- Roberts, G.A.F. 1992. *Chitin Chemistry*: Macmillan.
- Rojanarata, T., P. Opanasopit, S. Techaarpornkul, T. Ngawhirunpat, and U. Ruktanonchai. 2008. "Chitosan-thiamine pyrophosphate as a novel carrier for siRNA delivery." *Pharm Res* 25 (12):2807-14.
- Saraee, Mahdieh B., and Moharam H. Korayem. 2015. "Dynamic simulation and modeling of the motion modes produced during the 3D controlled manipulation of biological micro/nanoparticles based on the AFM." *Journal of Theoretical Biology* 378:65-78.
- Saraswat, P., R. R. Soni, A. Bhandari, and B. P. Nagori. 2009. "DNA as Therapeutics; an Update." *Indian Journal of Pharmaceutical Sciences* 71 (5):488-98.
- Sato, T., T. Ishii, and Y. Okahata. 2001. "In vitro gene delivery mediated by chitosan. effect of pH, serum, and molecular mass of chitosan on the transfection efficiency." *Biomaterials* 22 (15):2075-80.
- Scholz, Claudia, and Ernst Wagner. 2012. "Therapeutic plasmid DNA versus siRNA delivery: Common and different tasks for synthetic carriers." *Journal of Controlled Release* 161 (2):554-65.
- Senturk, S., M. Mumcuoglu, O. Gursoy-Yuzugullu, B. Cingoz, K. C. Akcali, and M. Ozturk. 2010. "Transforming growth factor-beta induces senescence in hepatocellular carcinoma cells and inhibits tumor growth." *Hepatology* 52 (3):966-74.
- Seymour, L. W., R. Duncan, J. Strohalm, and J. Kopecek. 1987. "Effect of molecular weight (Mw) of N-(2-hydroxypropyl)methacrylamide copolymers on body distribution and rate of excretion after subcutaneous, intraperitoneal, and intravenous administration to rats." *J Biomed Mater Res* 21 (11):1341-58.
- Shahidi, F., and R. Abuzaytoun. 2005. "Chitin, chitosan, and co-products: chemistry, production, applications, and health effects." *Adv Food Nutr Res* 49:93-135. doi: 10.1016/s1043-4526(05)49003-8.
- Siu, Y. S., L. Li, M. F. Leung, K. L. Lee, and P. Li. 2012. "Polyethylenimine-based amphiphilic core-shell nanoparticles: study of gene delivery and intracellular trafficking." *Biointerphases* 7 (1-4):16. doi: 10.1007/s13758-011-0016-4.
- So, A. Y., J. W. Jung, S. Lee, H. S. Kim, and K. S. Kang. 2011. "DNA methyltransferase controls stem cell aging by regulating BMI1 and EZH2 through microRNAs." *PLoS One* 6 (5):e19503.

- Stephen, A.M. 1995. *Food Polysaccharides and Their Applications*: Taylor & Francis.
- Taniyama, Y., J. Azuma, Y. Kunugiza, K. Iekushi, H. Rakugi, and R. Morishita. 2012. "Therapeutic option of plasmid-DNA based gene transfer." *Curr Top Med Chem* 12 (15):1630-7.
- Teoh, S.H. 2004. *Engineering Materials for Biomedical Applications*: World Scientific Pub.
- Thomas, Wirth, and Ylä-Herttuala Seppo. 2011. "Gene Therapy of Glioblastoma Multiforme - Clinical Experience on the Use of Adenoviral Vectors." In.
- Tong, H., S. Qin, J. C. Fernandes, L. Li, K. Dai, and X. Zhang. 2009. "Progress and prospects of chitosan and its derivatives as non-viral gene vectors in gene therapy." *Curr Gene Ther* 9 (6):495-502.
- Varkouhi, A. K., M. Scholte, G. Storm, and H. J. Haisma. 2011. "Endosomal escape pathways for delivery of biologicals." *J Control Release* 151 (3):220-8.
- Wagner, E. 1999. "Application of membrane-active peptides for nonviral gene delivery." *Adv Drug Deliv Rev* 38 (3):279-89.
- Wang, J., Z. Lu, M. G. Wientjes, and J. L. Au. 2010. "Delivery of siRNA therapeutics: barriers and carriers." *Aaps j* 12 (4):492-503. doi: 10.1208/s12248-010-9210-4.
- Wen, Z. S., L. J. Liu, Y. L. Qu, X. K. Ouyang, L. Y. Yang, and Z. R. Xu. 2013. "Chitosan nanoparticles attenuate hydrogen peroxide-induced stress injury in mouse macrophage RAW264.7 cells." *Mar Drugs* 11 (10):3582-600.
- Whitehead, Kathryn A., Robert Langer, and Daniel G. Anderson. 2009. "Knocking down barriers: advances in siRNA delivery." *Nat Rev Drug Discov* 8 (2):129-38.
- Wiley, John. 2013. "Gene Therapy Clinical Trials Worldwide".
<<http://www.abedia.com/wiley/years.php>> (updated July, 2015).
- Wimardhani, Y. S., D. F. Suniarti, H. J. Freisleben, S. I. Wanandi, N. C. Siregar, and M. A. Ikeda. 2014. "Chitosan exerts anticancer activity through induction of apoptosis and cell cycle arrest in oral cancer cells." *J Oral Sci* 56 (2):119-26.
- Wirth, Thomas, Nigel Parker, and Seppo Ylä-Herttuala. 2013. "History of gene therapy." *Gene* 525 (2):162-9.
- Wnek, G.E., and G.L. Bowlin. 2004. *Encyclopedia of Biomaterials and Biomedical Engineering*: Taylor & Francis.
- Xu, Y., and Y. Du. 2003. "Effect of molecular structure of chitosan on protein delivery properties of chitosan nanoparticles." *Int J Pharm* 250 (1):215-26.
- Yang, M. H., S. S. Yuan, Y. F. Huang, P. C. Lin, C. Y. Lu, T. W. Chung, and Y. C. Tyan. 2014. "A proteomic view to characterize the effect of chitosan nanoparticle to hepatic cells: is chitosan nanoparticle an enhancer of PI3K/AKT1/mTOR pathway?" *Biomed Res Int* 2014:789591.
- Yao, Q., W. Liu, X.J. Gou, X.Q. Guo, J. Yan, Q. Song, F.Z. Chen, Q. Zhao, C. Chen, and T. Chen. 2013. "Preparation, characterization, and cytotoxicity of various chitosan nanoparticles." *Journal of Nanomaterials* 2013.

- Young, J. I., and J. R. Smith. 2001. "DNA methyltransferase inhibition in normal human fibroblasts induces a p21-dependent cell cycle withdrawal." *J Biol Chem* 276 (22):19610-6. doi: 10.1074/jbc.M009470200.
- Zhang, Liyan, and Shantha L. Kosaraju. 2007. "Biopolymeric delivery system for controlled release of polyphenolic antioxidants." *European Polymer Journal* 43 (7):2956-66.
- Zhou, Y., J. Li, F. Lu, J. Deng, J. Zhang, P. Fang, X. Peng, and S. F. Zhou. 2015. "A study on the hemocompatibility of dendronized chitosan derivatives in red blood cells." *Drug Des Devel Ther* 9:2635-45. doi: 10.2147/DDDT.S77105.
- Ziegler, D. V., C. D. Wiley, and M. C. Velarde. 2015. "Mitochondrial effectors of cellular senescence: beyond the free radical theory of aging." *Aging Cell* 14 (1):1-7. doi: 10.1111/acel.12287.

APPENDIX A

MEDIA AND BUFFERS FOR THE TRANSFORMATION OF pKINDLING-RED-MITO

SOB Broth (For 1 liter)

Bacto tryptone	20.0 g
Bacto yeast extract	5.0 g
NaCl	0.6 g
KCl	0.5 g
MgCl ₂	10 mM
MgSO ₄	10 mM

Dissolve tryptone, yeast extract, sodium chloride, and potassium chloride in a final volume of 990 ml distilled H₂O and sterilize by autoclaving. Just prior to using, add 10 ml of magnesium stock (as below) to the SOB broth to make the media 20 mM with respect to magnesium.

Transformation Buffer 1 (500 ml)

RbCl	6.0 g
MnCl ₂ ·4H ₂ O	5.0 g
Potassium acetate	15.0 ml (1 M stock, pH 7.5)
CaCl ₂ ·2H ₂ O*	0.75 g
Glycerol	75.0 ml

Combine reagents above in dH₂O and adjust pH to 5.8 with 0.2 M acetic acid. Bring to final volume of 500 ml with dH₂O. Sterilize by filtration through a 0.22 µm disposable filter. Store at 4°C.

Transformation Buffer 2 (500 ml)

MOPS	10.0 ml (0.5 M stock, pH 6.8)
RbCl	0.6 g
CaCl ₂ ·2H ₂ O*	5.5 g
Glycerol	75.0 ml
dH ₂ O	to 500.0 ml

Combine reagents in dH₂O. Bring to a final volume of 500 ml with dH₂O. Sterilize by filtration through a 0.22 µm disposable filter. Store at 4°C.

* If using anhydrous CaCl₂ use 0.57 g for Buffer 1, and 4.15 g for Buffer 2.

2 M Mg²⁺ stock (100 ml)

MgCl ₂	20.3 g
MgSO ₄	24.7 g

Dissolve reagents in a final volume of 100 ml dH₂O. Sterilize by filtration through a 0.45 µm disposable filter. The resulting solution is 2 M with respect to Mg²⁺.

0.5 MOPS (100 ml)

Dissolve 10.47 g MOPS in dH₂O. Adjust pH to 6.8 with NaOH. Bring to final volume of 100 ml. Sterilize by filtration through a 0.22 µm disposable filter. MOPS buffer should be clear and colorless.

1 M Potassium acetate (100 ml)

Disolve 9.82 g potassium acetate in dH₂O. Adjust pH to 7.5 with acetic acid. Bring to final volume of 100 ml. Sterilize by autoclaving.

APPENDIX B

MEDIA AND SOLUTIONS FOR *IN VITRO* STUDIES

B.1. Media for Cell Cultures

A) *RPMI-1640 Growth Medium*: Roswell Park Memorial Institute – 1640 (RPMI 1640) growth medium, fetal calf serum (FCS), antibiotic and antimycotic mixed solution (100 U/ml penicillin, 0.1 mg/ml streptomycin and 0.25 mg/ml amphotericin B) were obtained from Department of Biotechnology, University of Rzeszów, POLAND.

<u>For 500 ml RPMI-1640</u>	50 ml FCS (~10%)	50 µg/ml antibiotic and antimycotic solution (~1%)
-----------------------------	------------------	--

B) *DMEM Growth Medium*: Dulbecco's modified Eagle's medium (DMEM) growth medium, fetal calf serum (FCS), antibiotic and antimycotic mixed solution (100 U/ml penicillin, 0.1 mg/ml streptomycin and 0.25 mg/ml amphotericin B) were obtained from Department of Biotechnology, University of Rzeszów, POLAND.

<u>For 500 ml DMEM</u>	50 ml FCS (~10%)	50 µg/ml antibiotic and antimycotic solution (~1%)
------------------------	------------------	--

B.2. MTT Reaction Solution

MTT reaction was prepared in PBS for the concentration of 5mg/ml. Each 96-well plate 3-(4,5-Dimethylthiazol-2-yl)-2,5-diphenyltetrazolium bromide was prepared as % 10 MTT solution with growth medium.

APPENDIX C

REAGENTS AND SOLUTIONS FOR THE DETERMINATION OF THE SENESCENCE-ASSOCIATED β -GALACTOSIDASE ACTIVITY (SA- β -gal)

Fixation Buffer:

Formaldehyde	703 μ l
Glutaraldehyde	52 μ l
PBS	12.245 μ l

Staining Buffer:

Citrid Acid Buffer	2.6 ml
X-gal pH 6	650 μ l
$K_4Fe(CN)_6$	650 μ l
$K_3Fe(CN)_6$	650 μ l
NaCl	390 μ l
$MgCl_2 \cdot 6H_2O$	26 ml
H_2O	8.034 ml

*This ratios are for total amount of 13 ml sample.

APPENDIX D

REAGENTS AND GEL PREPARATION FOR WESTERN BLOTTING

D.1. Standard Curve for BSA

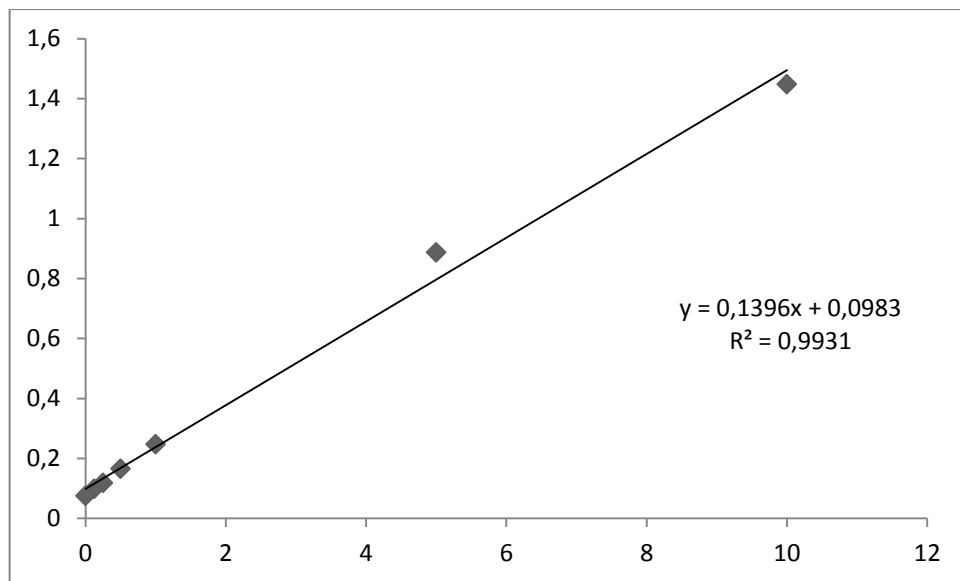


Figure D.1. Absorbance Values for BSA Standards

D.2. Reagents and materials

Stacking (resolving) Gel 3,9%		
Acrylamide/Bis-acrylamide (30%)	650 μ l	1,3 ml
0.5 M Tris-HCl, pH 6.8	1,25 ml	2,5 ml
10% SDS	50 μ l	100 μ l
deionized water	3 ml	6 ml
10% APS	25 μ l	50 μ l
TEMED	5 μ l	10 μ l

For a 30ml separating gel:

Separating Gel 10%		
Acrylamide/Bis-acrylamide (30%)	5 ml	10 ml
0.5 M Tris-HCl, pH 6.8	3,75 ml	7,5 ml
10% SDS	150 µl	300 µl
deionized water	6,1 ml	12,2 ml
10% APS	50 µl	100 µl
TEMED	10 µl	20 µl

* APS and TEMED must be added right before each use.

5x Running Buffer:	1x Running Buffer:
0,125 M Tris-HCl	25 mM Tris
0,92 M Glycine	192 mM Glycine
0.5% SDS	0,1 % SDS

Preparation of Transfer buffer (TOWBIN) :

For 1Liter (10X)

250 mM Tris	30,25g
1920 mM Glycine	144 g
20% Methanol (add fresh and cool in the -20°C)	

Working Concentration:

1 portion 10x TOWBIN buffer	2 portions of Methanol	7 portions of distilled water
------------------------------------	-------------------------------	--------------------------------------

TBST (Tris-buffered saline with TWEEN 20):

20 mM Tris-HCl pH 7,5	20ml
137 mM NaCl	137ml
0,1% Tween 20	1ml

* Complete to 1 L with dH₂O

** For Blocking Buffer %1 Bovine serum albumin (BSA) in TBST